ELSEVIER

Composites Science and Technology 62 (2002) 1489–1514

COMPOSITES SCIENCE AND TECHNOLOGY

www.elsevier.com/locate/compscitech

Biaxial test results for strength and deformation of a range of E-glass and carbon fibre reinforced composite laminates: failure exercise benchmark data

P.D. Soden[a], M.J. Hinton[b], A.S. Kaddour[c,*]

[a]*Mechanical Engineering Department, UMIST, Manchester, M60 1QD, UK*
[b]*Future Systems Technology Division, QinetiQ, Fort Halstead, Sevenoaks, Kent, TN14 7BP, UK*
[c]*Structures and Materials Centre, FST, QinetiQ, Farnborough, Hampshire, GU14 0LX, UK*

Abstract

In Part A of the World Wide Failure Exercise (published in *Composite Science and Technology*, Vol 58, No 7, 1998), all contributors were given exactly the same set of material properties and were asked to predict the strength and deformation of the same set of laminates under a range of specified loading conditions. In this part (Part B) of the exercise, available experimental results are superimposed on the theoretical predictions and returned to the contributors for comment. The test data were for (a) 0° unidirectional laminae under biaxial direct and shear loads (b) $(90°/\pm30°)_s$, $(0°/\pm45°/90°)_s$, $(\pm55°)_s$ multi-directional laminates under biaxial loads and (c) stress strain curves for $(0°/\pm45°/90°)_s$, $(\pm55°)_s$, $(\pm45°)_s$ and $(0°/90°)_s$ laminates under uniaxial and biaxial loads. This paper briefly describes the experimental results issued in Part B of the Exercise and their origin and limitations. Comments are made on the material properties given for the unidirectional fibre reinforced layers and constituents used in Part A of the Exercise and on approximations in the laminate models specified in Part A. © QinetiQ Ltd. 2002.

Keywords: Failure exercise

1. Introduction

The present paper is one of a series of papers related to the world wide failure exercise, which was launched in order to determine the accuracy of current theories for predicting failure in composite laminates. That has been achieved by comparing the predictions of 12 different failure theories with experimental data. This paper presents the experimental data and comments on the experiments. It was issued to all the participants in the failure exercise before they compared their theoretical predictions with the experimental results.

The experimental data covered 14 test cases involving (a) 0° unidirectional laminae under biaxial direct and shear loads (b) $(90°/\pm30°)_s$, $(0°/\pm45°/90°)_s$, $(\pm55°)_s$ multi-directional laminates under biaxial loads and (c) stress strain curves for $(0°/\pm45°/90°)_s$, $(\pm55°)_s$, $(\pm45°)_s$ and $(0°/90°)_s$ laminates under uniaxial and biaxial loads.

It has been noted that whilst there is a considerable body of experimental data describing the strength and mechanical response of composites, there appears to be a relatively limited number of studies where a wide range of loading conditions have been applied to the same laminate. This is partly due to the difficulties involved in such experiments.

Almost all of the experimental results chosen for use in this exercise were derived from tests on tubular specimens. Testing of tubes avoids problems associated with free edge effects that are encountered with coupon and other specimens and a wide range of biaxial and triaxial stresses can be applied by subjecting tubular specimens to combinations of internal or external pressure, torsion and axial load. The testing of tubular specimens can, however, involve problems including:-

- The avoidance of failures at end constraints and end fittings and the minimisation of end effects.
- Tubular specimens can experience various forms of buckling when they are subjected to circumferential or axial compression or torsion loading.

* Corresponding author. Tel.: +44−1252-395978; fax: +44−1252-395077.

E-mail address: askaddour@Qinetiq.com (A.S. Kaddour); mjhinton@Qinetiq.com (M.J. Hinton); peter.soden@umist.ac.uk (P. D. Soden).

0266-3538/02/$ - see front matter © QinetiQ Ltd 2002.
PII: S0266-3538(02)00093-3

- Tubes may exhibit changes in geometry during loading but these effects are usually ignored when processing experimental results.

Tubular specimens can fail in a variety of ways. Unless otherwise stated the specimens considered here failed by fracture. Some results are given for leakage failures in cases where the specimens were subjected to internal pressure. Very few experimental results are available for 'initial' failure, or the onset of damage such as resin cracking. In some cases the initial failures have no obvious effect on the mechanical behaviour of the structure but in other cases 'initial' failure may be expected to influence the shape of the stress–strain curves and for this reason contributors were asked to predict the shape of stress–strain curves.

In most cases all of the experimental results selected for any given set of loading cases were from tests carried out by the same investigators in the same laboratory. References are given to the sources of the experimental data and, where possible, to publications giving more details of the specimens and test procedures for each set of experiments.

Each specimen was tested to failure at a fixed ratio (**SR**)[1] of circumferential to axial stresses in the test section and the loads were usually increased continuously until fracture occurred. Unless otherwise stated the applied stresses were calculated based on initial (undeformed) tube dimensions with no allowance made for change of shape during loading.

The laminated tubes were constructed from unidirectional fibre reinforced composite plies. The ply angle θ is specified as the angle between the fibre direction and the axis of the tube. Note that $\theta = 90^\circ$ represents the circumferential direction and σ_y (or σ_θ) and σ_x are the applied stresses in the circumferential and the axial directions, respectively.

Unless otherwise stated the fibre volume fraction in the laminated specimens is approximately the same as the unidirectional laminae (UD) provided in Part A. The cure procedure followed that recommended by the resin manufacturers and was the same as for the UD laminates in Part A.

Whenever possible, the material properties issued in Part A were obtained from publications by the same investigators who tested the laminates presented here. In some cases, the investigators had employed the same materials in experimental studies of different laminates.

Sources of discrepancy between the predictions and the experimental results include combinations of the following:

(I) Errors and approximations in the theory.
(II) Errors in the experimental results.
(III) Errors in the given material properties.
(IV) Differences between the model laminates specified for analysis and the construction of the specimens used in the experiments.

The following sections present the experimental data for each of the laminates, comment on the source of the unidirectional laminate data presented in Part A and discuss some of the assumptions in the laminate models.

2. Description of experimental data for the exercise

2.1. Biaxial failure envelope for unidirectional E-glass/epoxy lamina under combined transverse and shear loading (σ_x versus τ_{xy}) (Fig. 10 of the failure exercise)

The results were given by Hütter et al. [1], and were obtained from experiments on circumferentially wound filament wound tubes. The tubes were 60 mm internal diameter, 2 mm thick and were constructed from 62% by volume Vetrotex 21×K43 E-glass fibre (Gevetex) rovings and a Ciba Geigy epoxy resin system LY556/HT907/DY063 mixed in weight proportions of 100:85:4. The tubes were cured at 100 °C for 2 h and post cured at 150 °C for 2 h.

The tubes were tested under torsion combined with axial tension or compression and the biaxial data are shown in Fig. 1 and listed in Table 1. Details of the tests are given in by Hütter et al. [1]. Also shown in Fig. 1 are the data supplied to contributors for use in their analysis. This data was taken from the original results presented in an earlier paper by the originators of the biaxial test program, Krauss and Schelling [2], and do not agree exactly with the strength obtained from the other test data presented in Fig. 1 which were reported by Hütter et al. [1].

2.2. Biaxial failure envelope for unidirectional T300/914C carbon/epoxy lamina under combined longitudinal and shear loading (σ_y versus τ_{xy}), Fig. 11 of the exercise

The results of Schelling and Aoki, [3,4], are used in the exercise. The specimens were in the form of axially wound tubes made from prepreg T300/BSL914C carbon/epoxy. The tubes were tested under combined axial tension or compression and torsion. All the tubes were end reinforced and grips were used to transmit the torque to the tubes.

One set of tubes was tested under combined axial tension and torsion. The results (Fig. 2), showed that the shear failure stresses tended to increase when simultaneous moderate axial tension stress was applied and decreased at higher tensile stresses.

[1] Similar definition of stress ratio is used when the loading involves normal and shear stresses.

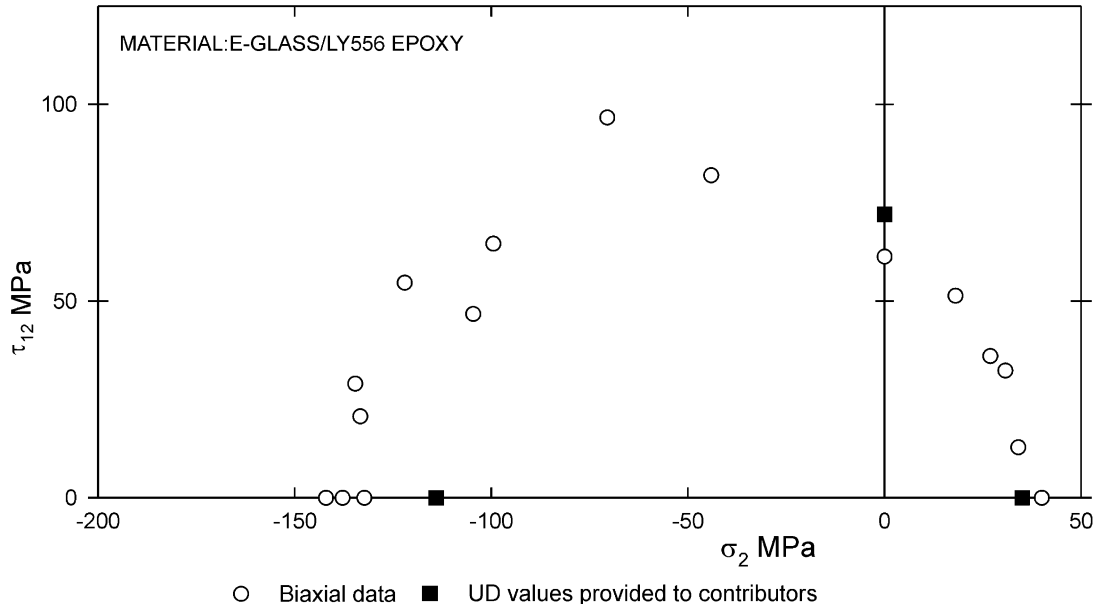

Fig. 1. Biaxial failure stress envelope for 0° unidirectional lamina made glass/epoxy under transverse and shear loading (σ_y versus τ_{xy}).

Table 1
Data for biaxial failure stresses of 0° unidirectional lamina under combined transverse and shear loading (σ_y versus σ_{xy}). Data for Fig. 10[a] of the failure exercise [1]

Axial stress σ_y (MPa)	Shear stress σ_{xy} (Mpa)
40.0	0.0
26.9	36.0
30.7	32.3
34.0	12.8
18.0	51.3
−137.8	0.0
−142.0	0.0
−132.3	0.0
−104.6	46.7
−134.6	28.9
−99.4	64.5
−70.5	96.6
−122.0	54.6
−44.1	81.9
−133.3	20.7
0.00	61.2

[a] Figure numbers refer to those given in Part A of the exercise.

Tests under combined axial compression and torsion were carried out at two laboratories on tubes of similar materials. The tubes were 32 mm in diameter and 1.9–2.3 mm thick. The results are plotted in Fig. 2 and the data used are listed in Table 2. A wide range of scatter is seen in the shear strength, when no axial load was applied. No explanation was available for the apparently different values between the shear strengths obtained from tension/torsion and compression/torsion data sets when no axial load was applied.

The volume fraction of fibres, $V_f = 0.56$, measured by Deutschen Forschungs und Versuchsanstalt für Luft- und Raumfarht (DFVLR) for the specimens used in the combined tension and shear tests is slightly lower than that given in Part A of the Exercise

2.3. Biaxial failure envelope for unidirectional lamina under combined longitudinal and transverse loading (σ_y versus σ_x), Fig. 12 of the exercise

The results reported by Al-Khalil et al. [5], were selected for this failure envelope. Most of the results were obtained from testing nearly circumferentially wound tubes under combined internal pressure and axial load. The winding angle, measured from the axial direction of the tubes, was ±85° rather than 90°. The specimens tested were filament wound glass/epoxy tubes produced by QinetiQ (formerly known as The Defence Evaluation and Research Agency (DERA), Fort Halstead, Kent, UK). The specimens were 100 mm inner diameter, 300 mm long and approximately 0.95 mm (2 covers[2] or 1.2 mm (3 covers) thick. The tubes were made of E-glass/epoxy material with a volume fraction of fibres approximately 0.6. The E-glass fibre reinforcement was Silenka 051L, 1200 tex and the epoxy resin system was Ciba-Geigy MY750/ HY917/ DY063 mixed in weight proportions of 100:85:2. The curing cycle was 2 h at 90° C followed by 1.5 h at 130 °C and 2 h at 150° C. The ends were reinforced with circumferentially wound E-glass fibre reinforced epoxy resin, leaving an un-reinforced test section 60 mm long. A rubber lining was applied to the inside surface of the specimens.

The tubes were tested under combined internal pressure and axial compression using the technique described

[2] See Section (4) for comments on filament wound tube construction.

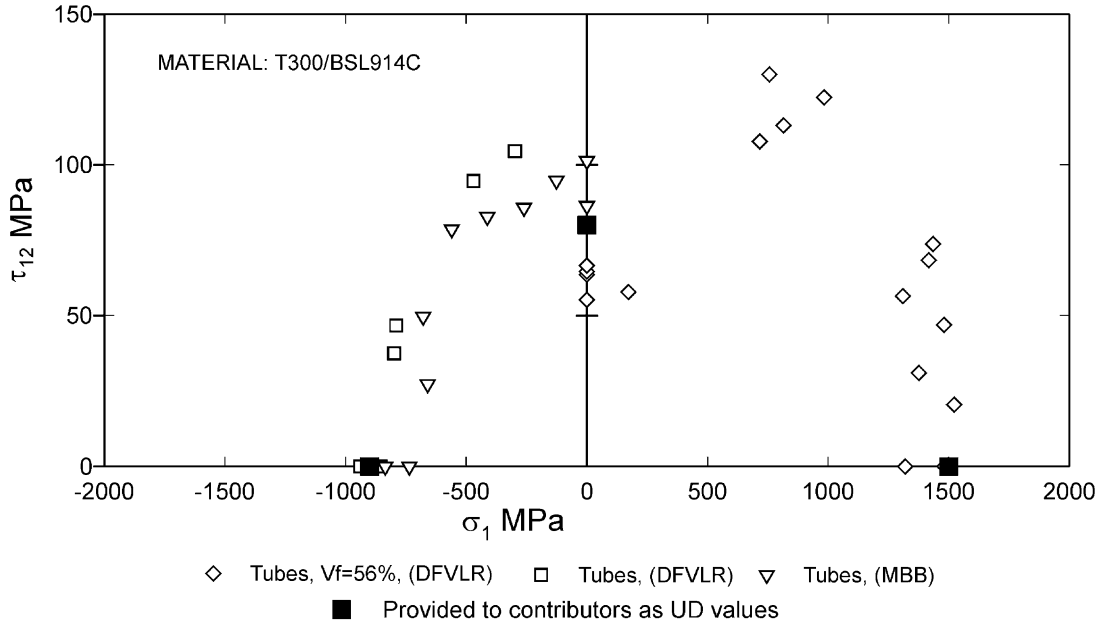

Fig. 2. Biaxial failure stress envelope for 0° unidirectional lamina made of T300/BSL914C under longitudinal and shear loading (σ_x versus τ_{xy}).

by Soden et al. [6,7]. During the tests, the pressure was increased at a steady rate (typically 2 MPa/min) and the axial load was increased continuously to maintain a constant predetermined ratio of applied hoop to axial stresses within the gauge length until the specimen fractured. The tubes were tested under ten different stress ratios. Eight specimens were tested at a nominal stress ratio **SR** = 1:0 and the stress–strain curves, measured at this stress ratio, were linear up to failure.

The test results are shown in Fig. 3 together with the tension and compression strengths in directions parallel and perpendicular to the fibres which were measured by different methods and were issued as basic properties for the unidirectional composite lamina.

The hoop σ_θ and axial σ_x stresses were calculated from the measured pressure P and axial load F using:

$$\sigma\theta = \frac{PR_i}{h} \tag{1}$$

and

$$\sigma_x = \frac{PR_i}{h} + \frac{F}{2\pi R_i h} \tag{2}$$

where R_i is the inner radius of the un-deformed tubes and h is the mean thickness. Eqs. (1) and (2) ignore any change in diameter. However, in plotting the failure stresses, correction was made for the axial tensile stress which arises at large displacements due the diameter at the centre of the gauge length becoming greater than the diameter at the ends of the tubes, Al-Khalil et al. [5]. The corrected data are listed in Table 3.

2.4. Biaxial failure envelope of (±30°/90°) E-glass/epoxy laminates under biaxial stress loading, Figs. 13 and 14 of the exercise.

Extensive work was reported by Krauss and Schelling [2], Forster and Knappe [8] and Hütter et al. [1], on the failure behaviour of $(90°/\pm30°/90°)_s$ E-Glass/LY556/HT907/DY063 epoxy tubes under combined pressure and axial load and combined torsion and axial load. Details of the material used are described in Section 2.1 above. The tubes were made by wet filament winding and had a volume fraction of fibres 0.62. The tubes were 60 mm inside diameter and 2 mm thick and had a gauge length of 80 mm for tests involving axial compression and 180 mm in tests involving axial tension. They were end reinforced and tested with a liner inside. The wall thickness consisted of two circumferentially wound (90°) layers, one at the inside and the other at the outside of the tube, and hellically wound ±30° central layers. The thickness of the 90° circumferential layers was 17.2% and the +30° and −30° layers together made up 82.8% of the total thickness of the tubes. Therefore, the material is not quasi-isotropic and the strength depends on the loading direction.

Tables 4 and 5 show the data points for failure under combined direct stresses (σ_y versus σ_x) and for failure under combined torsion and axial load (σ_x versus τ_{xy}). Figs. 4 and 5 show the failure stresses under combined axial and circumferential loading and under combined axial load and torsion, respectively, see and Hütter et al. [1]. All the specimens tested under internal or external pressure were lined with a flexible adhesive liner. No data was available on initial failure or leaking and all the data are for final rupture. The few test results carried out

Table 2
Data for biaxial failure stresses of 0° unidirectional lamina under combined longitudinal and shear loading (σ_y versus σ_{xy}). Data for Fig. 11 of the failure exercise [3,4]

Hoop stress σ_y (MPa)	Shear stress σ_{xy} (MPa)
1. Tests at DFVLR, tubes (V_f=0.56)	
1318.9	0.0
1481.1	0.0
1500.7	0.0
1522.8	20.4
1376.1	31.0
1480.6	46.9
1309.8	56.4
1417.3	68.4
1435.4	73.7
−983.4	122.3
−815.6	113.0
−716.2	107.7
−756.9	129.9
−172.2	57.8
−0.0	55.2
−0.0	63.5
−0.0	64.6
−0.0	66.5
2. Tests at DFVLR on tubes (D=32 mm, h=1.9–2.3 mm)	
−297.8	104.5
−469.4	94.6
−790.1	46.7
−798.7	37.4
−854.8	0.0
−939.3	0.0
3. Tests at MBB on tubes with D=32 mm, h=2.2 mm	
0.0	86.3
0.0	101.3
−126.0	94.7
−260.3	85.7
−412.4	82.7
−559.6	78.6
−678.3	49.6
−659.9	27.2
−735.6	0.0
−835.7	0.0

under external pressure and axial compression were reported to be governed by buckling.

2.5. Biaxial failure envelope of angle ply ±55° E-glass/epoxy laminates, Fig. 15 of the exercise

The specimens tested were filament wound glass/epoxy tubes produced by QinetiQ (formerly known as The Defence Evaluation and Research Agency (DERA), Fort Halstead, Kent, UK), see Section 2.3 above for material description. A simple ±55° helical winding pattern with a single winding angle was employed. (The winding angle is measured between the fibre direction and the tube axis.) The tubes were either 100 or 51 mm inner diameter and were of various thicknesses, see Table 6(a)–(c). The mean thickness was determined from measurements taken at 40 positions around the surface of each specimen. The fibre volume fraction measured using burn-off tests was approximately 60% for the thin tubes used for determining strength of the tension-tension quadrant of the failure envelope shown in Fig. 6 but higher for thick tubes.

The tubular specimens tested under combined internal pressure and axial load were 100 mm inside diameter, typically 1 mm (2 cover) thick and the overall length 300 with 60 mm gauge length. The ends of the tubes were reinforced and fitted with special grips. The test rigs and technique used were described by Soden et al. [6,7]. Some of the tests were carried out without a flexible plastic liner [Table 6(a)] and some with [Table 6(b)]. The specimens tested with a liner all failed by rupture. Some of the tubes tested exhibited significant damage and deformation before the final fracture (e.g. see Section 2.6). Most of the specimens tested without a liner failed by weeping or jetting of the test liquid (oil) through the tube wall [Specimens that failed in this way are identified in Table 6(a)]. Full test results for all the thin walled tubes have been documented in detail by Soden et al. [6,7]. Some of the thin walled tubes which were tested under axial compression failed by buckling and these results have been replaced with new results for thicker walled tubes that failed by bursting rather than buckling (see Table 6).

For biaxial compression tests which include testing thick tubes, the overall lengths of the 100 and 51 mm diameter specimens were 370 and 185 mm, respectively. In most of the tests the ratio of the specimens inside radius : wall thickness (R_i:h) was 5 and in some of the tests the specimens wall thickness was increased to evaluate the influence of shell buckling. The mean values of the volume fraction of fibres was V_f=0.68. The ends of the specimens had additional reinforcement and inner end plug contours carefully designed to avoid end failures and excessive stress concentrations. No outer grips were needed in the biaxial compression tests. The test techniques have been described by Kaddour and Soden [9], and the results which are listed in Table 6(c) and plotted in Fig. 6 have been described in detail by Kaddour et al. [10]. Almost all the tubes were tested without using any liner or elastomeric coating. Only one test was carried out using an elastic coating on the outer surface and the behaviour of the tube was similar to the others. All the tubes for which the results are plotted failed by rupture and not by buckling.

2.6. The stress–strain curve for ±55° angle ply laminate under uniaxial tension σ_y:σ_x=*SR*=1:0, (Fig. 16), and ***SR***=2:1 (Fig. 17) of the exercise

The stress–strain curves under uniaxial tension σ_y:σ_x=1:0 and σ_y:σ_x=2:1, used in the exercise, were taken from the work of Al-Khalil [11], at UMIST. The

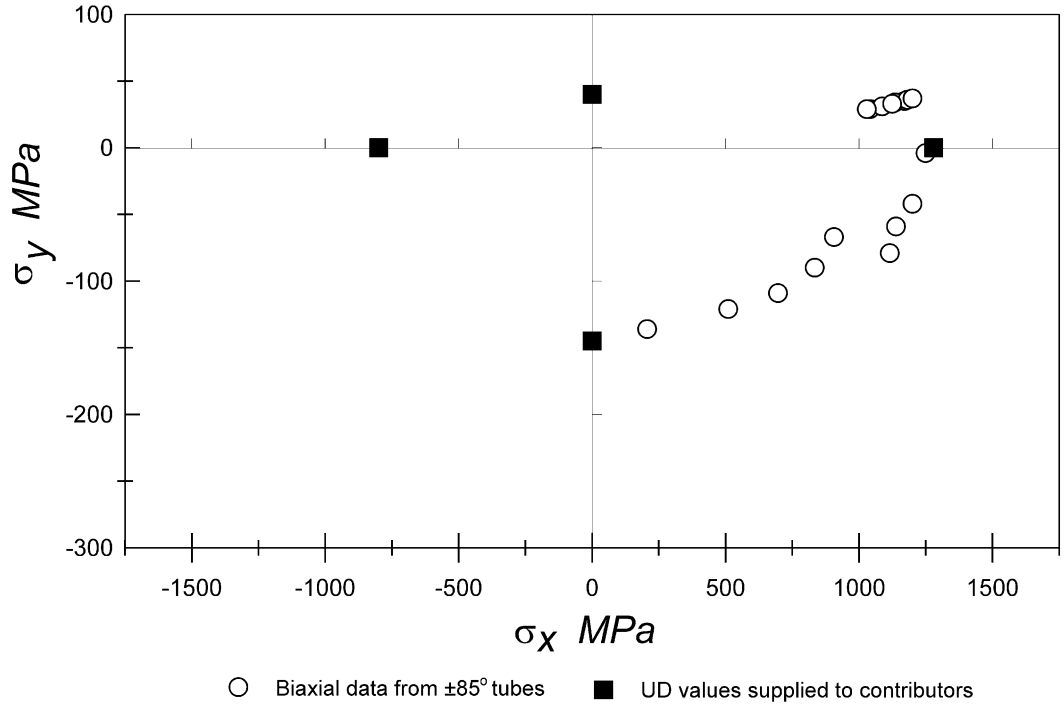

Fig. 3. Biaxial failure envelope of 0° GRP lamina under combined σ_x and σ_y stresses. Material: E-glass/MY750 epoxy.

Table 3
Data for biaxial failure stresses of nearly unidirectional (±85°) lamina under combined longitudinal and transverse loading (σ_y versus σ_x) for Fig. 12 of the failure Exercise. The results were taken from Table 1 of Al-Khalil et al. [5], unless otherwise stated

Hoop stress σ_y (MPa)	Axial stress σ_x (MPa)
0.0	40.0[a]
1280.0[b]	0.0
−800.0[c]	0.0
1170.0	35.0
1041.0	29.0
1134.0	34.0
1086.0	31.0
1181.0	36.0
1029.0	29.0
1200.0	37.0
1124.0	33.0
1249.0	−4.0
1200.0	−42.0
1138.0	−59.0
1115.0	−79.0
906.0	−67.0
834.0	−90.0
696.0	−109.0
510.0	−121.0
206.0	−136.0
0	−145.0[d]

[a] From axial tension tests on hoop wound tubes.
[b] From internal pressure tests on hoop wound tubes.
[c] This result was obtained from axial compression test on small cylindrical specimens.
[d] This was obtained from tests on hoop wound tubes under axial compression.

laminates used for testing ±55° E-glass/epoxy tubes were fabricated by wet filament winding. These tubes were of the same materials and were produced by the same manufacturer as those used for the biaxial envelope (Fig. 6) and for the ±85° tubes, see Section 2.3 above.

The tubes were 100 mm inner diameter, 310 mm overall length, 60 mm gauge length and typically 1 mm thick and a fibre volume fraction of 0.6. The actual tube construction consists of four plies (2 covers) with fibre directions at 55°/−55°/55°/−55°, relative to tube axis. The tubes were end reinforced with circumferentially wound E-glass/epoxy material and were tested under internal pressure. The test equipment and procedures used by Al-Khalil [11], were similar to those described by Soden et al. [6,7]. The hoop stress σ_θ (σ_y) was calculated using Eq. (1) and thus no allowance was made for bulging or change in dimensions of the tube under pressure.

The strains were measured at the mid-section of the outer surface by bonding three or four pairs of electrical resistance strain-gauges in the axial and circumferential directions. There was a considerable (up to ±20%) variation in the readings from individual strain gauge readings. The stress–strain curves presented are obtained from selected gauges.

2.6.1. Data for **SR** = 1:0 (Fig. 16 of the exercise)

The circumferential tension (**SR** = 1:0) tests were carried out with and without plastic liners using the test rig shown in Fig. 7(a). Loose pistons with low friction seals

Table 4
Biaxial failure stresses for (±30°/90°) E-glass/epoxy laminates under combined hoop and axial loading. Data for Fig. 13 of the failure exercise[1]

Axial stress σ_x (MPa)	Hoop stress σ_y (MPa)
292.3	312.0
592.3	157.5
730.8	385.5
557.7	269.3
720.5	384.0
548.7	405.0
−266.7	67.5
−268.0	66.0
−264.6	36.0
628.2	277.5
605.1	222.0
664.1	102.0
39.9	−107.2
−179.2	−82.4
223.8	−78.4
110.3	−91.2
−183.3	−78.4
−348.5	−40.0
483.7	−44.8
144.4	299.0
61.60	335.4
667.3	344.1
148.8	315.6
616.0	129.6
471.0	336.0
−164.2	195.0
−195.1	138.0
−115.5	247.5
48.70	301.5
633.9	157.5
577.5	202.5
385.0	351.0
474.8	312.0
577.2	0.0
535.2	0.0
531.3	0.0
559.5	0.0
605.7	0.0
531.3	0.0
559.5	0.0
−346.5	0.0
−354.2	0.0
0.0	291.0
0.0	267.0
0.0	289.5
0.0	−113.6
0.0	312.0

Table 5
Biaxial failure stresses for (±30°/90°) E-glass/epoxy laminates under combined axial load and torsion. Data for Fig. 14 of the failure exercise [1]

Axial stress σ_x (MPa)	Shear stress σ_{xy} (MPa)
577.2	0.0
531.3	0.0
282.3	228.9
436.3	140.1
513.3	100.8
462.0	173.4
410.7	251.2
64.2	199.9
128.3	222.1
128.3	248.6
192.5	274.2
256.7	284.5
−346.5	0.0
−354.2	0.0
0.0	233.2
320.8	258.9
320.8	261.4
38.5	231.5
256.7	278.5
102.6	198.2
154.0	211.0
205.3	218.7
308.0	283.6
359.3	206.7
359.3	216.2
410.7	159.8
462.0	120.5
513.3	15.4
535.2	0.0
−256.7	194.8
0.0	265.7
−64.2	271.7
−154.0	240.9
−308.0	138.4
−333.7	75.2
−38.5	238.4
−102.7	269.1
−154.0	227.3
−192.5	223.8
−282.3	162.3
−308.0	145.2
531.3	0.0
559.5	0.0
605.7	0.0

were fitted into the end of the tube. The pressure end load acting on the pistons was carried by tie bars and not by the specimen. The axial loads due to seal friction and due to bulging of the specimen under pressure were neglected.

Table 7 gives the data for hoop stress, hoop strain and axial strain used for plotting the stress–strain curves and the typical stress–strain curves for SR = 1:0 chosen for the exercise are shown in Fig. 8. These were taken from a test on a lined specimen carried out by Al-Khalil [11]. The failure hoop stress was approximately 595 MPa, the hoop failure strain 8.8% and the axial failure strain—10.9%. The mean failure hoop strain, using 6 strain—gauges on two specimens, was 8.7±1.2 (%). The mean axial strain, using 6 strain-gauges on two specimens, was −12.1±1.6%. (The selected axial strain curve was at the lower strain bound of the results.)

The failure stress for this specimen is consistent with the results used to plot the biaxial failure envelope for the ±55° tubes and with other results by Al-Khalil [11] and Soden et al. [6], for the same stress ratio of 1:0 on

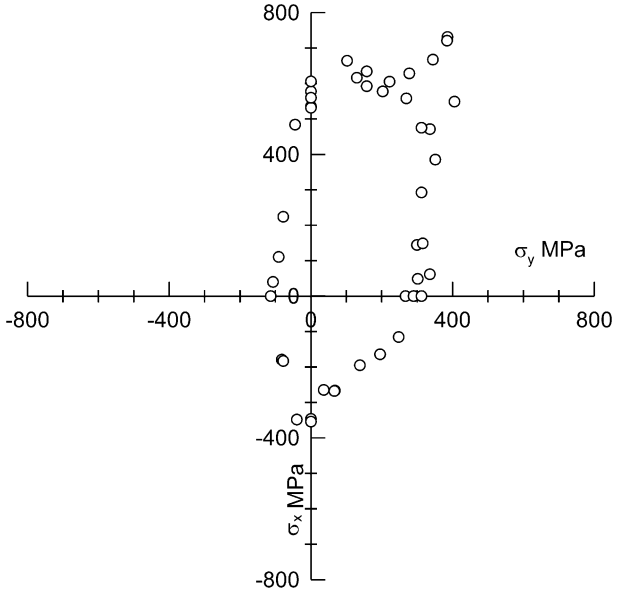

Fig. 4. Biaxial failure stress envelope for (90°/±30°/90°) laminate made of Glass/epoxy under combined loading (σ_y versus σ_x).

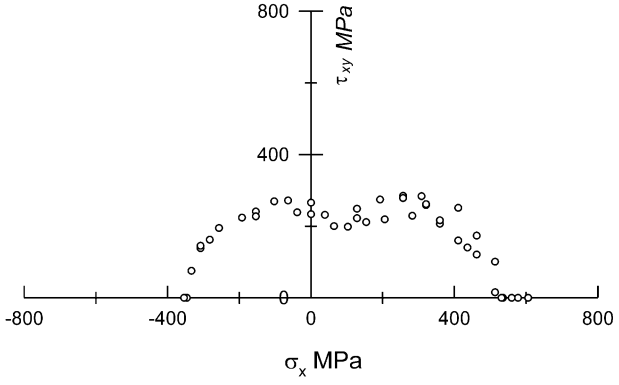

Fig. 5. Biaxial failure stress envelope for (90°/±30°/90°) laminate made of Glass/epoxy under combined loading (σ_x versus τ_{xy}).

lined specimens. The strength of unlined specimens for use in the exercise is 386 MPa. This value was taken from the work of Soden et al. [6], who reported two test values of 362 and 410 MPa for unlined tubes which failed by oil jetting through the wall thickness, and it is consistent with the mean strength of unlined tubes reported by Al-Salehi et al. [12], on tubes without end reinforcement which was 427±13 MPa. In the latter work, the failure strains of unlined tubes were $\varepsilon_y = 4.36 \pm 0.61\%$ and $\varepsilon_x = -4.85 \pm 0.44\%$, which are also in agreement with those selected for the exercise and marked in Fig. 8.

2.6.2. Data at *SR* = 2:1 (Fig. 17 of the exercise)

The specimens were tested under internal pressure with the ends closed using the rig shown in Fig. 7(b). The axial stress was taken to be half of the hoop stress, i.e. **SR** = 2:1. The stress–strain curves chosen for the Exercise are shown in Fig. 9. These were typical curves taken from one test on a lined specimen carried out by

Table 6a
Biaxial test results of ±55° GRP tubes subjected to combined internal pressure and axial loading

Hoop stress σ_y (MPa)	Axial stress σ_x (MPa)	Type of failure
69.0	92	[S]
106.0	106.0	[S]
137.0	116.0	[S]
134.0	103.0	[S]
197.0	124.0	[5]
209.0	122.0	[S]
300.0	151.0	[S]
271.0	135.0	[S]
302.0	151.0	[S]
268.0	134.0	[S]
491.0	196.0	[S]
615.0	205.0	[S]
852.0	257.0	[F]
775.0	234.0	[F]
820.0	234.0	[J]
736.0	133.0	[J]
605.0	0.0	[J]
362.0	0.0	[J]
410.0	0.0	[J]
321.0	−17.0	[J]
318.0	−17.0	[J]
191.0	−47.0	[G,S]
64.7	−129.0[a]	[J]
110.7	−112.5[a]	[J]
0.0	69.0	
0.0	76.0	

The tubes were 100 mm inside diameter and typically 1 mm thick and $V_f = 0.6$, unless otherwise shown [6]. Data for Fig. 15 of the failure exercise—tests carried out without using a liner.

[S]: Weeping (spots of oil).
[F]: Specimens fractured without initial failure.
[J]: Jetting of oil.
[G]: Combination of buckling and interlaminar shear.
[a] 5.1 mm thick specimen, $V_f = 0.68$.

Al-Khalil [11]. The failure hoop stress, computed using Eq. (1), was approximately 668 MPa. The hoop failure strain was 2.5%, which was very typical of other gauge readings. The axial failure strain was 4.2%, although other axial gauges gave strains as low as 3%. Table 8 gives the data for hoop stress, hoop strain and axial strain used for plotting the stress–strain curves. The specimens failed by extensive cracking parallel to and across the fibres, presumably due to transverse tension and fibre tension fractures in the gauge length.

Other tests were carried out in [6,11,13] at the same stress ratio of 2:1 and gave mean strengths of lined tubes as 684, 692 and 736 MPa, respectively. The mean strengths of unlined tubes reported by Soden et al. [6], and Kaddour et al. [13], which failed by oil leaking through the wall thickness, were 280 and 320 MPa, respectively. The strength of unlined and lined specimens shown in Fig. 9 are 280 and 736 MPa. These were taken from Soden et al. [6], and are the same as the strengths for the failure envelope in Fig. 6.

Table 6b
Biaxial test results of ±55° GRP tubes subjected to combined internal pressure and axial loading, Refs [6,11,13]

Hoop stress σ_y (MPa)	Axial stress σ_x (MPa)
0.0	74.0
0.0	62.0
107.0	143.0
198.0	198.0
331.0	280.0
374.0	288.0
525.0	332.0
599.0	349.0
723.0	365.0
736.0	368.0
741.0	370.0
717.0	358.0
750.0	375
835.0	334.0
803.0	321.0
914.0	305.0
939.0	283.0
867.0	262.0
921.0	263.0
817.0	148.0
761.0	138.0
676.0	67.0
516.0	0.0
594.0	0.0
638.0	0.0
622.0	0.0
544.0	0.0
492.0	−27.0
256.0	−65.0
114.3	−115.5[a]

The tubes were 100 mm inside diameter and typically 1 mm thick and $V_f = 0.6$, unless otherwise shown. Data for Fig. 15 of the failure exercise–-for tests carried out using a liner.

[a] 5.1 mm thick specimen, $V_f = 0.68$.

Table 6c
Details of biaxial test results of ±55° GRP tubes subjected to combined external pressure and axial compression [10]

Diameter mm	Thick. mm	σ_θ[b] (MPa)	σ_x[b] (MPa)
51	4.8	−680	−347
100	14.4	−709	−365
100[a]	14.3	−715	−366
51	7.13	−798	−409
51	8.82	−836	−430
51	10.0	−807	−417
51	8.77	−888	−457
100	9.43	2.5	−152
100	9.57	2.5	−149
51	4.78	−94	−195
51	4.94	−269	−273
51	4.65	−260	−267
51	4.76	−403	−329
51	4.66	−540	−320
51	4.67	−520	−352
51	7.13	−693	−406
100	9.595	−557	−235
100	9.9	−588	−249
51	5.87	−769	−312
51	5.2	−705	−282
51	4.24	−476	−174
51	4.78	−549	−186
51	4.73	−384	−96
100	9.51	−289	−57
51	4.64	−276	−42
100[c]	9.55	−339	−53

The tubes had a typical fibre volume fraction of 0.68. Data for Fig. 15 of the failure exercise. Tubes were of different diameters and thicknesses.

[a] This specimen was tested with rubber coating on the outside surface.

[b] These are the stresses at the inside surface.

[c] In this test, a special end plug was used which allows for the end pressure to be applied over the thickness of the specimen only. Therefore, the results of this test include some unknown friction.

The shape of the stress–strain curves in Fig. 9 is quite similar to that of other results for tests carried out at UMIST, although there was some variation in the axial strain readings [6,11,13]. The shape is different from that published by other investigators using different types of glass/epoxy and specimen geometry, see for instance [68,69].

2.7. Biaxial failure envelope of quasi-isotropic $(90°/\pm45°/0°)_s$ AS4/3501–6 tubes, Fig. 18 of the Exercise.

Biaxial behaviour of quasi-isotropic $(90°/\pm45°/0°)_s$ tubes made of AS4/3501–6 carbon/epoxy material was investigated by Swanson and Nelson [14], Swanson and Christoforou [15], Swanson and Colvin [16], and Colvin and Swanson [17]. The tests were carried out by subjecting the tubular specimens to pressure and axial loads.

The specimens used for testing AS4/3501-6 pre-preg material were fabricated by hand lay-up and autoclave cured at 177 °C. The wall construction was $(90°/\pm45°/0°)_{ns}$ where n was 1 for most tests, but was either 2, 3 or 4 for tests used to study the effect of wall thickness. Note that the 90° direction coincides with the circumferential direction of the tubes.

In most of the tests involving internal pressure loading, the tubes were 96 mm inside diameter, gauge length 80 mm. The total length of the specimens was 430 mm for standard tests and 330 mm for other tests that did not involve axial tension [18]. The specimens were end reinforced with fibre glass cloth over-wraps, aluminium ring and low modulus epoxy. A thin rubber bladder was used as a liner for tests involving internal pressure. The strains were measured using 3 strain-gauge rosettes, located around the mid-plane on the outer surface of the tubes.

The hoop σ_θ and axial σ_x stresses were calculated from the measured pressure P and axial load F using

$$\sigma_\theta = \frac{PR_m}{h} \tag{3}$$

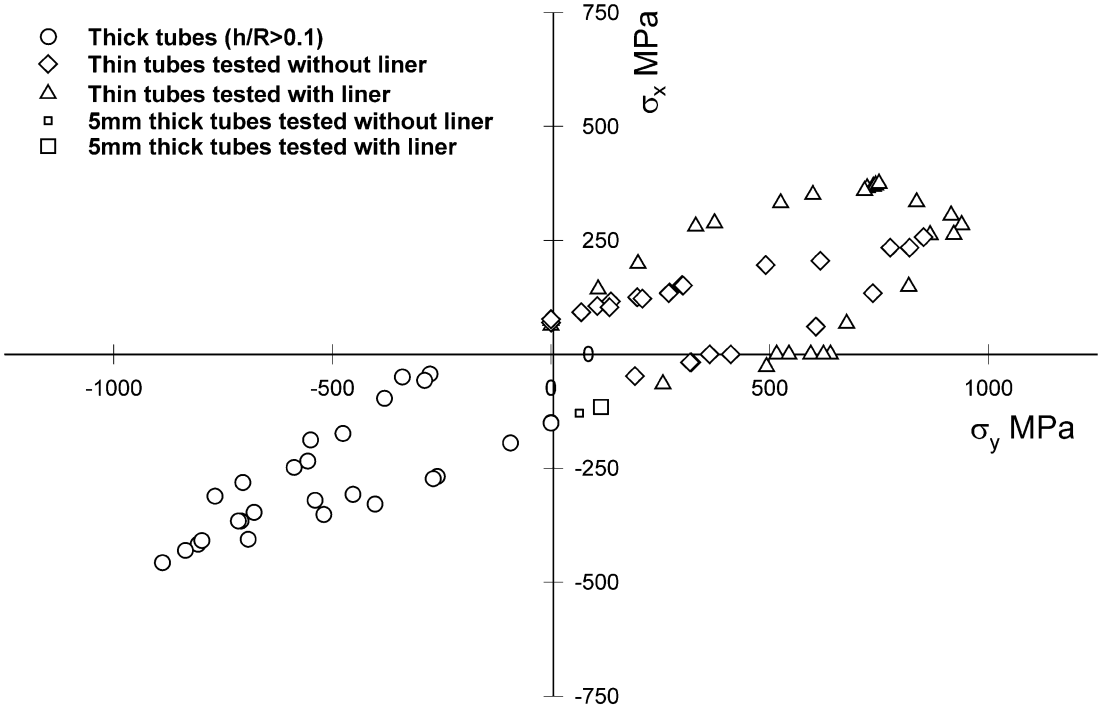

Fig. 6. Biaxial failure stress envelope for ±55° angle ply laminate made of Glass/epoxy under combined loading (σ_y versus σ_x).

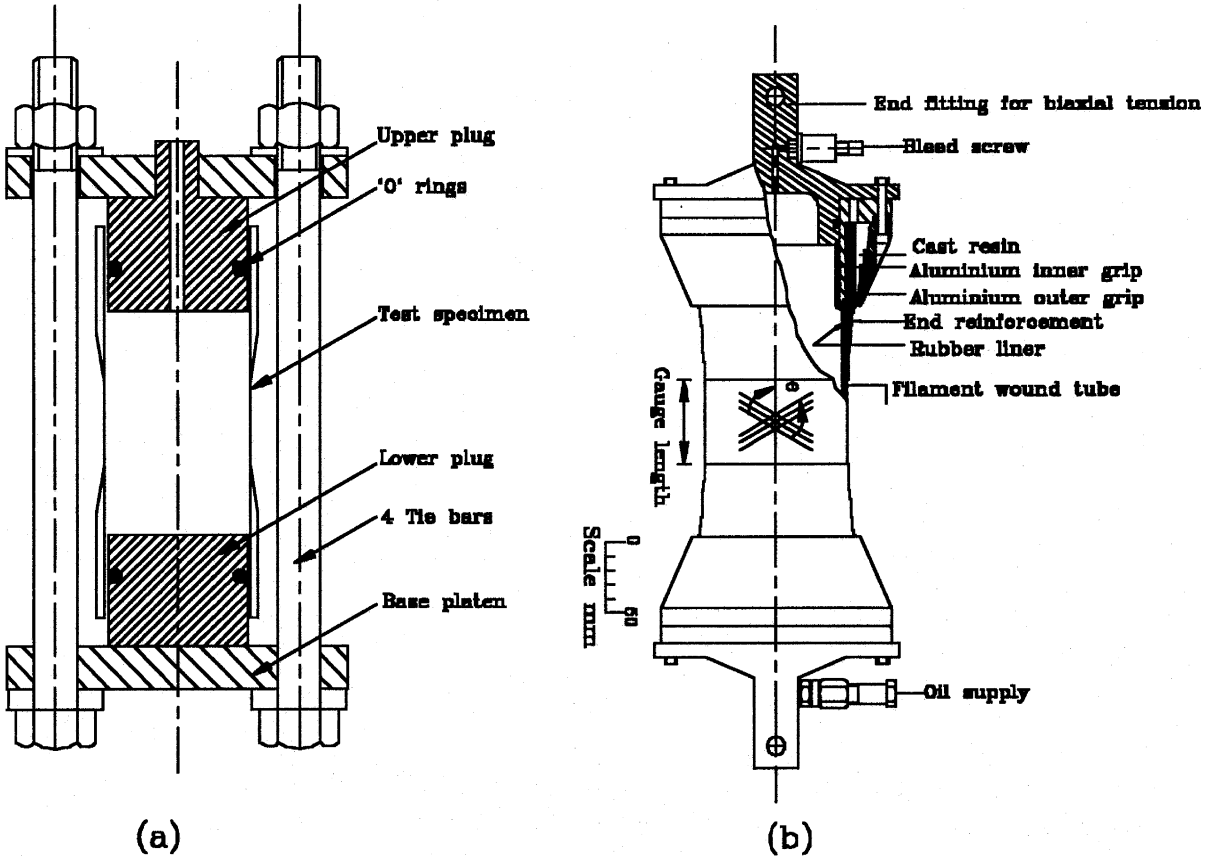

Fig. 7. Schematic diagrams of test rigs used in the biaxial tests ±55° and ±45° angle ply tubes: (a) For open end burst test, i.e. for SR = 1:0; (b) For SR = 2:1 and SR = 1:1 and others.

Table 7
Data for stress–strain curves for ±55° angle ply tubes made of E-glass/epoxy material tested under $\sigma_y:\sigma_x = 1:0$ [11]

Hoop stress σ_y (MPa)	Hoop strain ε_y (%)	Axial strain ε_x (%)
0.0	0.0	0.0
12.3	0.04	−0.01
25.2	0.12	−0.04
37.1	0.18	−0.07
51.4	0.26	−0.11
60.7	0.31	−0.14
75.4	0.39	−0.19
84.2	0.45	−0.23
95.2	0.52	−0.28
106.2	0.61	−0.34
121.6	0.72	−0.42
131.7	0.82	−0.49
144.6	0.94	−0.59
157.2	1.05	−0.68
164.8	1.14	−0.75
177.5	1.26	−0.85
191.3	1.40	−0.98
208.0	1.57	−1.13
215.1	1.69	−1.25
231.1	1.86	−1.40
244.7	2.04	−1.57
254.8	2.18	−1.71
269.3	2.37	−1.90
280.8	2.55	−2.09
289.0	2.68	−2.23
300.5	2.84	−2.40
309.9	3.01	−2.58
325.7	3.22	−2.80
338.7	3.42	−3.02
357.0	3.75	−3.40
368.1	3.92	−3.60
382.0	4.21	−3.95
394.3	4.43	−4.21
410.0	4.68	−4.49
423.4	4.97	−4.87
437.3	5.27	−5.27
475.5	6.11	−6.45
506.2	6.67	−7.27
522.4	7.10	−8.02
528.7	7.52	−8.81
557.4	8.03	−9.74
584.1	8.46	−10.41
594.9	8.78	−10.93

Data for Fig. 16 of the failure exercise.

and

$$\sigma_x = \frac{F}{A} \tag{4}$$

where R_m is the mean radius, h is the thickness and A is the cross sectional area of the tubes [15].

In addition to the 96 mm inner diameter tubes, tests were also carried out on 38 mm and 51 mm inner diameter tubes, Refs [16–17]. The 38 mm diameter tubes were tested under axial compression only while the 51 mm tubes were used to obtain failure strength data under external pressure with and without axial compression and under internal pressure only with no axial load.

The mean axial compressive strength of the 38 mm tubes was 637 MPa while that obtained from the 96 mm tubes was 375 MPa. No explanation was offered for the large difference in the results but Swanson and Colvin [16], hinted that buckling of the 96 mm tubes might have resulted in the corresponding low axial strength values.

The 51 mm tubes tested under internal pressure had a radius:thickness ratio (R:h) of 25 and those used for external pressure tests had R:h of 13. The final circumferential failure stress under internal pressure (**SR** = 1:0) was 721 MPa (tension) and that under external pressure (**SR** = -1:0) was 317 MPa (compression).

Fig. 10 shows the experimental failure stresses obtained from the different publications and the data for the axial and circumferential stresses are listed in Table 9.

The mode of failure for tests under hoop tension and axial loading was reported to be by fibre fracture, i.e. the final failure was dominated by the fibre strength. In some of the tests, a non-catastrophic failure took place prior to the final failure. The non-catastrophic (or initial) failure was in the form of softening behaviour of the stress–strain curves that followed initially linear behaviour. The softening response, which manifested itself in a change in the slope of the stress–strain curves, was attributed to matrix cracking [9]. Some of the data points of change in the slopes of the stress–strain curves reported by Swanson and Christoforou [20], and Trask [19], have been extracted and marked on the failure envelope in Fig. 10.

Buckling was observed to take place in the tests carried out under external pressure with and without axial compression. Therefore, the test results in the compression-compression quadrant represent structural failure by buckling rather than crushing failure of the material.

2.8. Stress–strain curve for quasi-isotropic (90°/±45°/0°)$_s$ AS4/3501–6 laminates under uniaxial tension $\sigma_y:\sigma_x = \boldsymbol{SR} = 1:0$, Fig. 19 of the exercise

The specimens were cut off from five feet long, hand laid up cylinders manufactured by Hercules Incorporated. The tubes were 96.5 mm inside diameter, approximately 1 mm thick, 80 mm gauge length and 419 mm total length. The tubes were similar to those employed by Swanson and his co-workers at the University of Utah (USA) in some of the experiments to determine the results used in the biaxial tension failure envelope for this laminate, see the previous section. The stress–strain curves (Fig. 11), under uniaxial tension $\sigma_y:\sigma_x = 1:0$, used in the exercise, originated from the work of Christoforou [21]. Christoforou tested a specimen

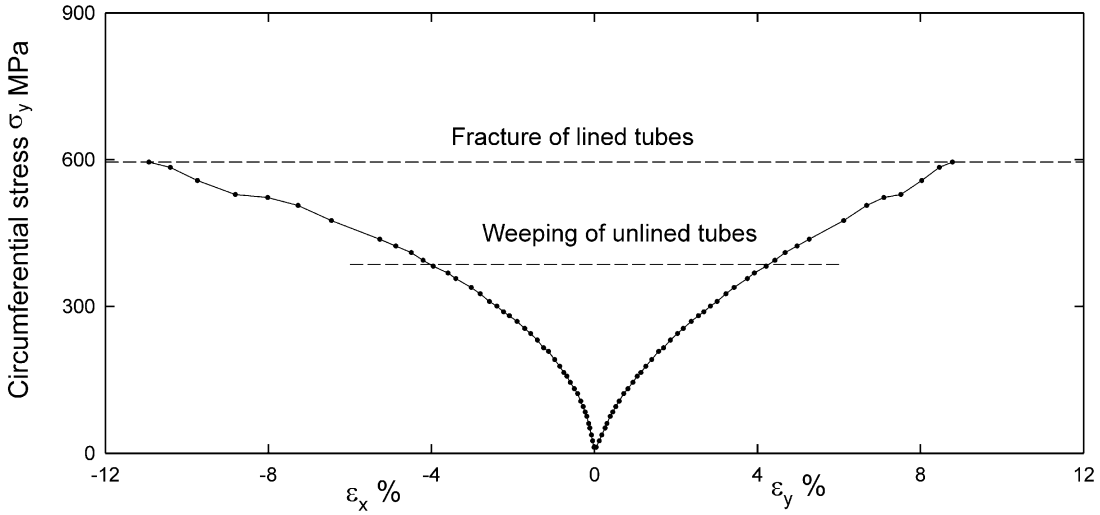

Fig. 8. Stress–strain curves for $\pm 55^\circ$ angle ply laminate made of Glass/epoxy under uniaxial tensile loading with $\sigma_y{:}\sigma_x = 1{:}0$.

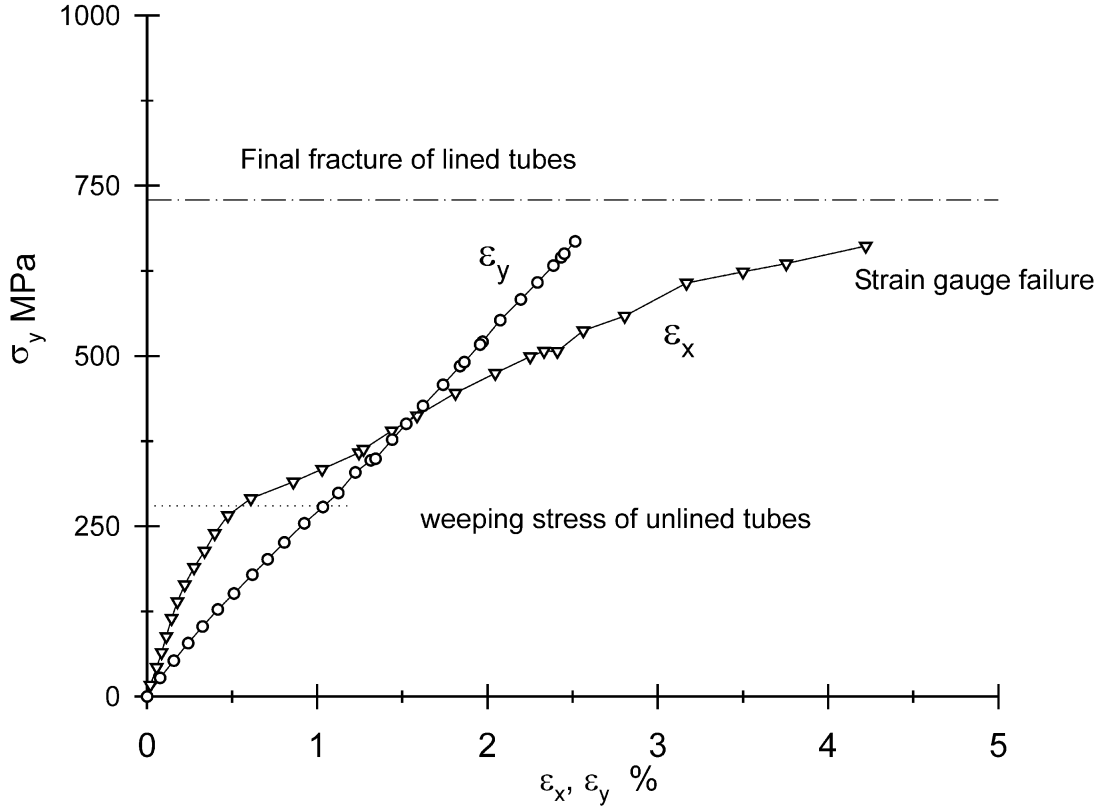

Fig. 9. Stress–strain curves for $\pm 55^\circ$ angle ply laminate made of Glass/epoxy under biaxial tensile loading with $\sigma_y{:}\sigma_x = 2{:}1$.

under internal pressure with no axial load. Due to friction at seals, the actual stress ratio was $\sigma_y{:}\sigma_x = 20{:}1$. The circumferential failure stress was 718 MPa and the hoop failure strain was 1.45% and the axial strain was −0.36%. Table 10 gives the data[3] for hoop stress-hoop strain and axial strain used for plotting the stress–strain curve [the circumferential stress was calculated using Eq. (3)]. The stress–strain curve under $\sigma_y{:}\sigma_x = 20{:}1$ was published by Swanson and Christoforou [20], but the co-ordinates used were σ_θ versus $\overline{Q}_{\theta\theta}\ \varepsilon_\theta + \overline{Q}_{\theta x}\ \varepsilon_x$. As pointed out by Swanson and Christoforou [20], the slope of such a curve is an identity, i.e. the slope makes an angle of 45° to the stress axis, if the material response is linearly elastic. The curve shows a decrease in the

[3] The data presented in the Table were obtained through personal communication with Professor S. R. Swanson who quoted Christoforou MSc thesis (1984) [21], as a source of information.

Table 8
Data for stress–strain curves for ±55° angle ply tubes made of E-glass/epoxy material tested under σ_y:σ_x = 2:1 [11]

Hoop stress σ_y (MPa)	Hoop strain ε_y (%)	Axial strain ε_x (%)
0.0	0.0	0.0
17.00	0.04	0.02
27.30	0.08	0.04
42.60	0.13	0.06
52.60	0.16	0.07
64.90	0.20	0.09
78.30	0.24	0.10
88.20	0.28	0.11
102.50	0.33	0.13
114.70	0.37	0.15
127.40	0.42	0.16
139.20	0.46	0.18
151.00	0.51	0.20
164.10	0.56	0.22
178.60	0.62	0.25
189.50	0.67	0.28
201.10	0.71	0.30
213.50	0.76	0.34
225.90	0.80	0.37
239.50	0.86	0.40
254.10	0.92	0.44
265.60	0.97	0.48
278.00	1.03	0.57
290.60	1.08	0.61
298.90	1.12	0.75
315.10	1.18	0.86
328.60	1.22	0.97
333.60	1.25	1.03
346.40	1.31	1.14
358.00	1.37	1.25
348.70	1.34	1.24
363.10	1.39	1.27
377.00	1.44	1.36
390.10	1.49	1.44
400.20	1.52	1.49
412.40	1.57	1.59
426.10	1.62	1.68
445.60	1.69	1.81
457.70	1.74	1.92
474.50	1.80	2.05
484.60	1.84	2.15
499.10	1.89	2.25
490.60	1.86	2.25
507.00	1.92	2.33
520.80	1.97	2.43
506.70	1.92	2.41
516.40	1.96	2.46
537.10	2.02	2.56
552.50	2.07	2.71
558.50	2.10	2.81
582.70	2.19	2.96
607.10	2.28	3.17
607.50	2.29	3.28
623.50	2.35	3.50
632.70	2.39	3.63
635.50	2.40	3.76
644.50	2.43	3.91
661.30	2.50	4.22
649.80		
637.70		
668.10		
668.30		

Data for Fig. 17 of the failure exercise.

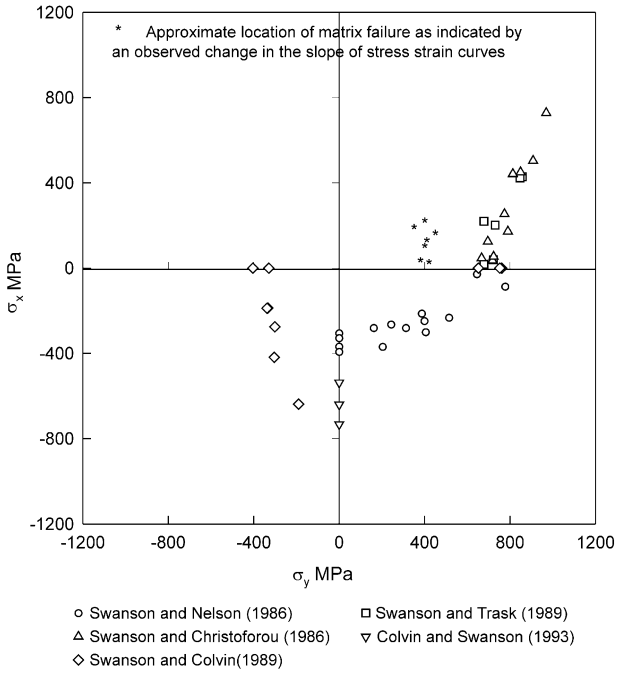

Fig. 10. Biaxial failure stress envelope for $(90°, \pm 45°, 0°)_s$ laminate made of AS4/3501–6 under combined loading (σ_y versus σ_x).

slope at around 400 MPa hoop stress indicating a form of initial failure in the laminate.

Other tests were carried out at a nominal stress ratio of 1:0, and occasionally the stress–strain curves were reported, Swanson and Trask [22], and Swanson and Colvin [16]. The mean strength reported by those investigators is 713 MPa (±42 MPa) which is close to the strength of 718 MPa used in the exercise. The scatter in the results is quite small (approximately ±5%).

2.9. The stress–strain curve for quasi-isotropic $(90°/\pm 45°/0°)_s$ AS4/3501-6 laminates under a stress ratio of ***SR*** *= 2:1, Fig. 20 of the exercise*

The specimens were similar to those used to obtain stress–strain curves under **SR** = 1:0 and also to those used for establishing the tension–tension biaxial envelope, described above. The stress–strain curves under biaxial tension σ_y:σ_x = 2:1 were from the work of Trask [19] at the University of Utah, USA. Trask tested two specimens under a stress ratio of **SR** = 2:1. The lay-up was described as $(90°/\pm 45°/0°)_{s2}$ and the exact ply consequence was $(90°/+45°/-45°/0°/0°/-45°/+45°/90°)$. The stress–strain curves were obtained from the various graphs reported by Trask. The hoop stress versus hoop strain curve was digitised from Fig. 4–14 of Trask [19], while the hoop stress versus axial strain curve had to be extracted from Trask's Figs. 4–21 and 4–30. The latter figures were for specimen number LTCU-86-1-#3 and were plotted by Trask as

Table 9
Biaxial failure stresses for quasi-isotropic $(90^\circ, \pm 45^\circ, 0^\circ)_s$ AS4/3501–6 laminates under a variety of stress ratios

Axial stress σ_x (MPa)	Hoop stress σ_y (MPa)	Remarks
The first set: tests on 96 mm tubes [14].		
−305.82	0.0	
−328.40	0.0	
−368.43	0.0	
−393.06	0.0	
−281.19	161.97	
−369.45	203.73	
−264.77	243.46	
−281.19	312.73	
−213.46	387.10	
−248.35	399.32	
−300.69	405.43	
−232.96	514.44	
−87.23	777.26	
−28.73	644.83	
The second set: tests on tubes (96 mm diameter, 1 mm thick) under internal pressure and axial load [22].		
Axial stress σ_y (MPa)	Hoop stress σ_x (MPa)	
428.7	857.4	
423.5	847.1	
38.70	721.9	
220.0	677.1	
202.0	730.5	
18.1	677.6	
The third set: tests on tubes (96 mm diameter, 1 mm thick) under internal pressure and axial load [15]		
Axial stress σ_x (MPa)	Hoop stress σ_y (MPa)	
46.90	667.0	
172.2	790.0	
35.80	718.0	
124.8	696.0	
54.5	723.0	
254.0	774.0	
450.0	849.0	
442.0	813.0	
504.0	908.0	
728.0	969.0	
The fourth set: tests on 38.1 mm diameter and approximately 2 mm thick tubes [17]		
Axial stress σ_x (MPa)	Hoop stress σ_y (MPa)	
−733.0	0.0	
−537.0	0.0	
−640.0	0.0	
The fifth set: tests on 51.8 mm diameter tubes [16]		
σ_x (MPa)	σ_y (MPa)	Remarks
0.0	652.0	$h = 1.05$ mm thick, internal pressure only
0.0	761.0	$h = 1.05$ mm thick, internal pressure only
0.0	752.0	$h = 1.05$ mm thick, internal pressure only
0.0	−404.0	$h = 2.11$ mm thick, external pressure only
0.0	−329.0	$h = 2.11$ mm thick, external pressure only
−418.0	−304.0	$h = 2.11$ mm thick, axial compression and external pressure, suspected circumferential buckling failure
−638.0	−190.0	$h = 2.11$ mm thick, axial compression and external pressure, failed at grips due to end brooming interaction
−275.0	−301.0	$h = 2.11$ mm thick, axial compression and external pressure, suspected circumferential buckling failure
−187.0	−334.0	$h = 2.11$ mm thick, axial compression and external pressure, suspected circumferential buckling failure
−188.0	−338.0	$h = 2.11$ mm thick, axial compression and external pressure, suspected circumferential buckling failure

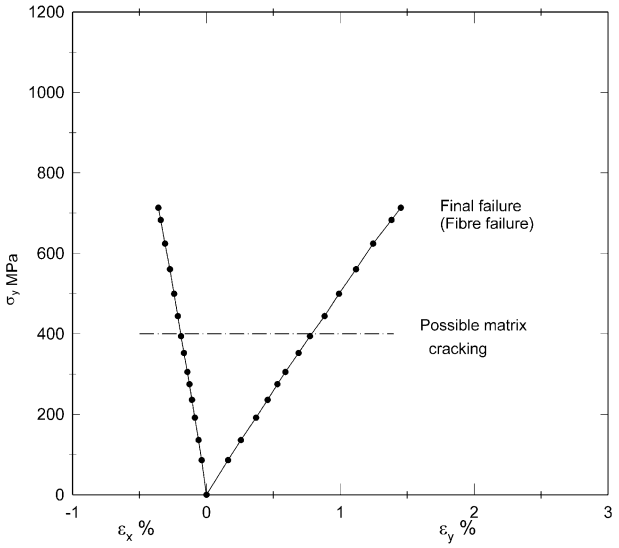

Fig. 11. Typical stress–strain curves for $(90^\circ, \pm 45^\circ, 0^\circ)_s$ laminate made of AS4/3501–6 under uniaxial tensile loading in y direction (σ_y:σ_x = 1:0).

Table 10
Data for stress–strain curves for quasi-isotropic $(90^\circ, \pm 45^\circ, 0^\circ)_s$ tubes made of AS4/3501–6 carbon/epoxy material tested under σ_y:σ_x = 20:1

Hoop stress σ_y (MPa)	Hoop strain ε_y (%)	Axial strain ε_x (%)
0.0	0.000	0.0000
47.1	0.084	−0.0175
86.0	0.161	−0.036
108.2	0.207	−0.047
135.8	0.257	−0.059
172.0	0.325	−0.076
191.5	0.370	−0.087
213.6	0.414	−0.098
235.8	0.457	−0.109
257.9	0.493	−0.118
274.7	0.530	−0.127
291.3	0.561	−0.136
305.2	0.589	−0.143
324.8	0.624	−0.152
352.4	0.688	−0.168
371.7	0.727	−0.179
394.0	0.773	−0.190
419.0	0.824	−0.203
444.1	0.882	−0.214
468.9	0.933	−0.227
499.5	0.990	−0.242
530.0	1.047	−0.256
560.5	1.117	−0.273
593.7	1.182	−0.291
624.1	1.245	−0.310
660.4	1.335	−0.331
682.7	1.382	−0.342
702.0	1.420	−0.352
713.1	1.452	−0.360
718.0	1.455	−0.363

Data for Fig. 19 of the failure Exercise. (The results taken from Table 6, page 68 of Christoforou [21], for specimen number QIL-3, see also Swanson and Christoforou [15].)

σ_θ(hoop stress) versus $\overline{Q}_{\theta\theta}\varepsilon_{\theta x}\varepsilon_x + \overline{Q}_{\theta x}\varepsilon_\theta$ and
σ_x(axial stress) versus $\overline{Q}_{\theta x}\varepsilon_\theta + \overline{Q}_{xx}\varepsilon_x$

where the values of the stiffness $\overline{Q}_{\theta\theta}$, $\overline{Q}_{\theta x}$ and $\overline{Q}_{xx}$ were measured for that specimen and given as $\overline{Q}_{\theta\theta}$ = 51.3 GPa, $\overline{Q}_{\theta x}$ = 18.9 GPa and $\overline{Q}_{xx}$ 60.2 GPa. The measured elastic properties and failure stresses of the two tubes were reported by Trask.

The stress–strain curves, back calculated from the graphs, are shown in Fig. 12s and the corresponding data are listed in Table 11. The response is linear at low strain levels but shows significant softening at higher strains. The non-linear behaviour starts at a strain between 0.6 and 0.8%. That corresponds to a change in the slope of stress–strain curves around 450 MPa hoop stress. Further reduction appears to take place at a hoop stress of 750 MPa. The final hoop strengths of two tubes tested by Trask [19], were 857 and 847 MPa.

2.10. The stress–strain curve for ±45° angle ply laminate under biaxial tension σ_y:σ_x = ***SR*** = *1:1, Fig. 21 of the exercise*

The specimens were in the form of ±45° tubes which were made by the same manufacturer (DRA) using the same material as for the ±55° tubes described earlier (Section 2.3). The stress–strain curves under biaxial tension σ_y:σ_x = 1:1, used in the exercise, were from the work of Li [23], and Reid et al. [24], at UMIST. The ±45° E-glass/epoxy tubes were fabricated by wet filament winding and cured at 120 °C. The specimens were two cover filament wound tubes and the tube wall consisted of four layers of E-glass/epoxy oriented at 45°/−45°/

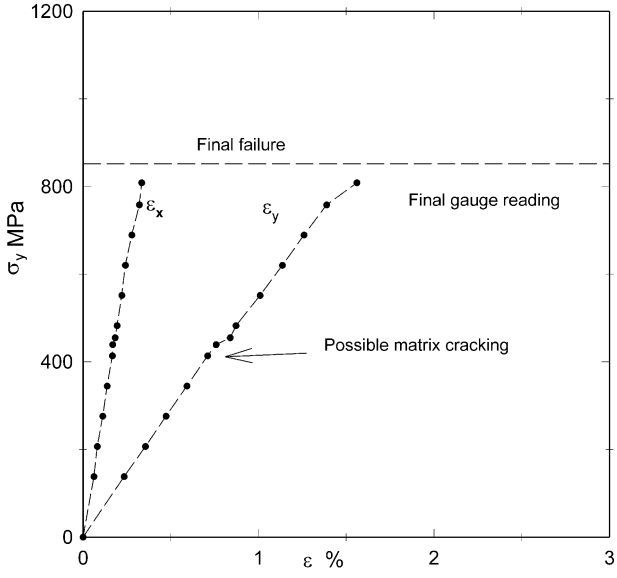

Fig. 12. Typical stress–strain curves for $(90^\circ, \pm 45^\circ, 0^\circ)_s$ laminate made of AS4/3501–6 under biaxial tensile loading with σ_y:σ_x = 2:1.

Table 11
Data for the stress–strain curves for quasi-isotropic $(90°,\pm45°,0°)_s$ tubes made of AS4/3501-6 carbon/epoxy material tested under **SR** = 2:1

Hoop stress σ_y (MPa)	Hoop strain ε_y (%)	Axial strain ε_x (%)
0.0000	0.0000	0.0000
137.8	0.2343	0.0621
206.7	0.3558	0.0814
275.6	0.4729	0.1124
344.5	0.5923	0.1376
413.4	0.7100	0.1669
438.9	0.7583	0.1689
454.8	0.8389	0.1828
482.3	0.8715	0.1939
551.2	1.0086	0.2208
620.1	1.1359	0.2408
689.1	1.2595	0.2777
758.0	1.3881	0.3208
808.3	1.5607	0.3345

Data for Fig. 20 of the failure Exercise. Data were extracted from the work of Trask [19].

45°/−45° to the tube axis. The tubes were 100 mm inner diameter, 310 mm overall length, 60 mm gauge length and typically 1 mm thick. The tubes were end reinforced and tested under internal pressure and axial load using the rig, Fig. 7(b), and test methods described by Soden et al. [6]. The tubes were tested under equal biaxial tension, i.e. the axial stress was equal to the hoop stress. The stresses were calculated using Eq. (1) and (2), i.e. no allowance made for the change of shape of the tube under load. The strains were measured at the mid-section of the outer surface by bonding electrical resistance strain-gauges in the axial and circumferential directions.

The stress–strain curves chosen for the exercise are shown in Fig. 13. These were selected from the results of one test on a lined specimen carried out by Reid et al. [24]. The final hoop stress was around 444 MPa and the corresponding hoop and axial strains were 2.47 and 2.17%, respectively. Table 12 gives the data for hoop stress, hoop strain and axial strain used for plotting the stress–strain curves.

Readings from individual strain gauges on 4 different specimens varied by up to 22%. One of the peculiar features of these results is that the hoop strains are larger than the axial strains, although ideally all the strains should be equal to each other [23]. Reasons for such divergence between the hoop and axial strains are not clear.

In some of these tests, the crack spacing was recorded from a series of photographs as the loading progressed. Cracks were observed for stresses as low as 50–70 MPa. The rate of crack growth tended to level out beyond a stress of approximately 200 MPa, which coincided closely with the observed failure stress (216 MPa) of an unlined specimen tested by Soden et al. [7]. The specimens failed by extensive cracking parallel to the fibres, presumably due to transverse tension and by fibre tension fractures in the gauge length.

The mean stress at which maximum strains were recorded was 419 MPa, but the strength of the tubes was believed to be higher than that. Other tests were carried out by Soden et al. [7] at the same stress ratio of **SR** = 1:1 on 3 lined tubes. The mean strength of these lined tubes which failed by rupture was 502 ± 35MPa [7]. The volume fraction of the fibres of similar tubes was 0.55. The strength of an unlined specimen, which failed by leakage was reported by Soden et al. [7] as 216 MPa . These values of hoop failure stresses (502 and 216 MPa) are marked in Fig. 13.

*2.11. The stress–strain curve for ±45° angle ply laminate under biaxial tension σ_y:σ_x = **SR** = 1:−1, Fig. 22 of the exercise.*

The stress–strain curves under biaxial loading σ_y:σ_x = 1:−1, used in the exercise, were from the work of Kaddour et al. [25] at UMIST and were generated from tests on ±45° filament wound tubes of the same E-glass/ MY750 epoxy material and manufactured by DRA. The tubes were 100 mm inner diameter, 370 mm overall length, 120 mm gauge length and typically 5.9 mm thick and had a fibre volume fraction of 0.6. The tubes were end reinforced and tested under internal pressure and axial compression. The test equipment was similar to that described by Soden et al. [7], but a large (500 kN) capacity machine was used to apply the axial loads and the ratio of internal pressure to axial compression was kept constant during the test. No end grips were used. The larger wall thickness for **SR** = 1:−1 specimens, compared with the **SR** = 1:1 tubes, was to avoid shell buckling under these axial loads. The inside surface hoop σ_θ and axial σ_x stresses were calculated from the measured pressure P and axial load F and the original tube dimensions using thick cylinder theory. The inside surface axial compressive stress was equal in magnitude to the inside surface tensile hoop stress in these tests.

The stress–strain curves chosen for the exercise are shown in Fig. 14 and were selected from the results of one lined specimen. At failure, the computed stress at the inside surface of the tubes was 94.8 MPa and the hoop failure strain was 9.9% and the axial failure strain was −11.2%. Table 13 gives the data for hoop stress, hoop strain and axial strain used for plotting the stress–strain curves. The strains were measured at the inside surface of the tubes.

2.12. Stress–strain curves for cross-ply $(0°/90°)_s$ laminate made of E-glass/epoxy material tested under σ_y:σ_x = 1:0, Fig 23 of the exercise

Work on characterising the behaviour of 90°/0° cross ply glass/epoxy has been carried out by a number of

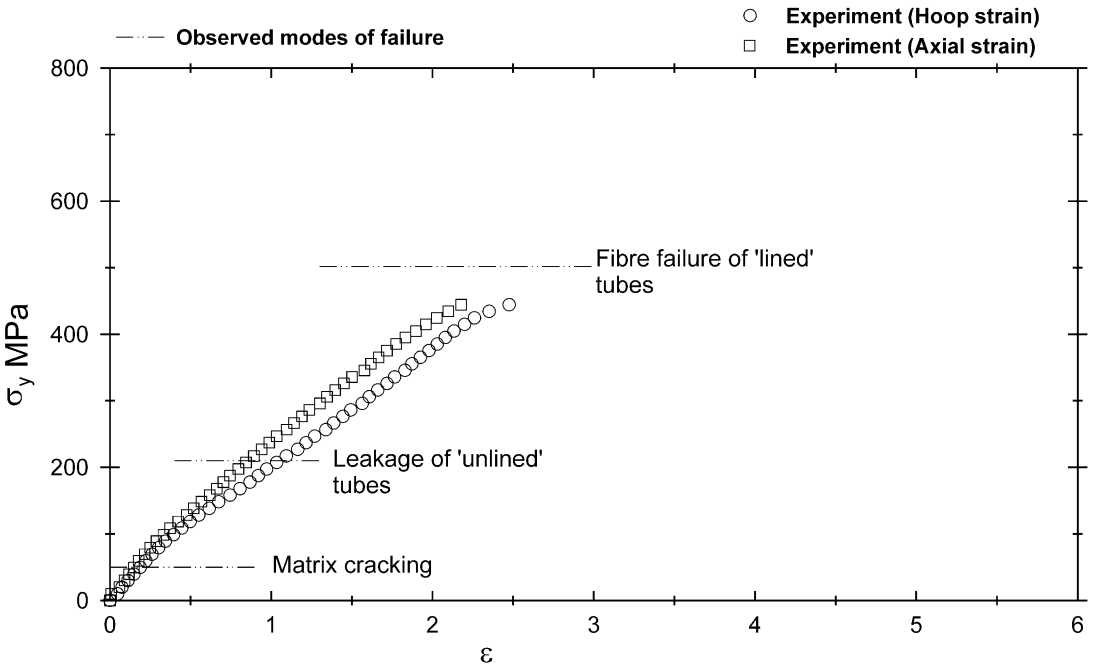

Fig. 13. Typical stress–strain curves for $\pm 45^\circ$ GRP angle ply laminate under biaxial tensile loading with $\sigma_y:\sigma_x = 1:1$.

investigators. Very recently, Eckold [26–28], and Hinton [29], obtained stress strain curves for cross ply laminates using different test specimens. In all of these specimens, particular attention was paid to observing and recording cracking of the laminates. Details are described below for the results of the two groups.

2.12.1. Results for tubes

One set of stress–strain curves under uniaxial tension $\sigma_y:\sigma_x = 1:0$ originated from the work of Eckold [27][4] at AEA Technology (Didcot, Oxon, UK). The specimens were in the form of the tubes of 150 mm inside diameter, 1.04 mm thick, 700 mm overall length and 620 mm gauge length. The lay up was $90^\circ/0^\circ/0^\circ/90^\circ$ where the 90° direction is the hoop direction. The material employed was similar to that used in testing the $\pm 45^\circ$ and $\pm 55^\circ$ winding angle tubes described above in Sections 2.3, 2.5 and 2.6, except that the matrix was MY750/HY 917/DY 070. The fibre volume fraction was typically 0.6. The tubes were end reinforced and tested under internal pressure with no axial load. The end load was carried by four tie bars and O ring and cup seals were used to prevent leakage from tube ends during pressurisation. No liner was used and the test was stopped when weeping occurred.

Whitening did not occur and individual transverse cracks in the 90 plies were formed which extended along the entire axial gauge length of the tubes. These cracks were clearly visible with minimal damage/ opacity extending beyond the cracks themselves. Cracks began at a hoop stress of approximately 175 MPa, Eckold [26,28], see Fig. 15.

The last available readings of the strains were at hoop stress of 323 MPa. At that stress, the hoop strain was 1.55% and the axial strain was −0.118%.

Failure took place by weeping through a delamination (remote from the ends) at a hoop stress of approximately 400 MPa and no fibre fracture occurred. Further details can be found in the work of Eckold [26] and Eckold et al. [28].

2.12.2. Results for coupons

QinetiQ (formerly known as The Defence Evaluation and Research Agency (DERA), Fort Halstead, Kent, UK) has also been engaged in obtaining a full characterisation of the behaviour of cross ply glass/epoxy laminate under uniaxial tension. The specimens tested were made of four layers oriented at $0^\circ/90^\circ/90^\circ/0^\circ$ relative to the loading direction (along the 0° direction), with an overall thickness of 1.9 mm and all the layers have an identical thickness of 0.475 mm. The coupons were 25 mm wide, 200 mm long and have a gauge length of 100 mm, leaving a 50 mm distance at each end for bonding end taps. The edges of the specimens were polished. The specimens were equipped with strain gauges in directions parallel to and the transverse to the loading direction. The material was similar to that of the 55° winding angle tubes (described in Sections 2.3, 2.5 and 2.6 of the data pack for Part B) except that the matrix was MY750/HY 917/DY 070. The fibre volume fraction was 0.62.

[4] Personal communication from Dr. G. C. Eckold. The results were obtained as a part of a collaborative project carried out by the National Physical Laboratory and AEA Technology, Harwell, within the "Materials Measurement Program"; a program of underpinning research financed by the UK Department of Trade and Industry.

Table 12
Data for stress–strain curves for ±45° angle ply tubes made of E-glass/epoxy material tested under σ_y:σ_x = 1:1

Hoop stress σ_y (MPa)	Hoop strain ε_y (%)	Axial strain ε_x (%)
0.0	0.0	0.01
19.80	0.0745	0.0584
29.91	0.1113	0.0911
39.66	0.1479	0.1174
49.75	0.1868	0.1483
59.59	0.2218	0.1785
69.52	0.2601	0.2149
79.25	0.3012	0.2492
89.12	0.3433	0.2871
98.88	0.3939	0.3313
108.79	0.4450	0.3716
118.66	0.4965	0.4226
128.41	0.5498	0.4762
138.26	0.6146	0.5188
148.31	0.6735	0.5670
158.27	0.7446	0.6196
168.12	0.8057	0.6617
177.78	0.8680	0.7037
187.65	0.9192	0.7442
197.47	0.9715	0.7958
207.34	1.0328	0.8437
217.11	1.0927	0.8918
227.20	1.1638	0.9398
237.01	1.2155	0.9869
246.93	1.2688	1.0334
256.73	1.3383	1.0950
266.57	1.3872	1.1411
276.55	1.4442	1.1898
286.40	1.4930	1.2351
296.25	1.5636	1.3021
306.13	1.6075	1.3465
316.22	1.6599	1.3962
326.11	1.7172	1.4503
335.91	1.7648	1.5017
345.76	1.8284	1.5778
355.57	1.8723	1.6183
365.46	1.9244	1.6665
375.50	1.9775	1.7175
385.27	2.0287	1.7745
395.06	2.0790	1.8326
404.98	2.1326	1.8971
414.77	2.1982	1.9589
424.67	2.2595	2.0261
434.47	2.3510	2.0976
444.42	2.4750	2.1780

Data for Fig. 21 of the failure Exercise, data taken from Ref [24].

A total of five tests were carried out and the mean final failure stress was 590 MPa, with a coefficient of variation of $CV = 11.8\%$. The, mean failure strain in the loading direction was $\varepsilon_x = 2.69\%$, with $CV = 14.4\%$, and that in the transverse direction was $\varepsilon_y = -0.13\%$, with $CV = 8.3\%$. Typical stress–strain curves are shown in Fig. 16. The onset of first crack was recorded at a strain of $\varepsilon_x = 0.375\%$ which corresponds to a load per unit area 117.5 MPa on the coupon. The onset of longitudinal splitting was observed at a strain of $\varepsilon_x = 1.3\%$ and that resulted in a small kink, not shown here, in the strain perpendicular to the loading direction. The coupons finally failed by fibre fracture. Table 14 presents data for the stress and both strains, along and perpendicular to the loading direction, measured in one typical specimen. The failure stress was 609 MPa and the failure strains were $\varepsilon_x = 2.69\%$ and $\varepsilon_y = 0.12\%$ along and perpendicular to the loading direction, respectively.

Eckold [28] also tested coupons of the same material and of similar construction and the stress at final failure (fibre fracture) was 598 MPa with a standard deviation of 47 MPa. This fracture strength is shown in Fig. 15. The full stress–strain curves up to final failure were not available at the time of writing. The results of Eckold on coupons are very similar to those of Hinton [29] (see Fig. 16).

2.12.3. Results to be used for the exercise

The original intention was to follow the policy of using the experimental results from tubes Fig. 15, but because complete stress–strain curves are available for coupons, the organsiers have chosen Hinton's results [29], for comparison with predictions. The data are listed in Table 14.

3. Properties for unidirectional layers and constituents

Details of the properties used in the laminate predictions were given in Part A [30], of the exercise. Properties for unidirectional layers were usually obtained from the same sources as the experimental data for the laminates used in Part B. In some cases where laminates of similar materials were tested in different laboratories the same set of material properties was employed to minimise the number of data sets issued. Inevitably not all of the required properties were available and then approximate values (sometimes arbitrary values) were employed.

Typical values of properties of four different unidirectional (UD) laminae used in Part A the Exercise were given by Soden et al. [30]. The four (UD) laminae are:

1- E-Glass/MY750 epoxy (Silenka E-glass/MY750/HY917/DY063)
2- E-Glass/LY556 epoxy (Gevetex E-glass/LY556/HT907/DY063)
3- AS4 Carbon/epoxy (AS4/3501–6)
4- T300 Carbon/epoxy (T300/BSL914C)

The data and their sources are discussed below.

3.1. Material I: E-glass/MY750/HY970/DY063

The data presented in Part A for this material were provided by Hinton [31], and were based on tests carried out on different specimens depending upon the property sought. The longitudinal tensile properties of the unidirectional fibre reinforced material in the direction parallel to

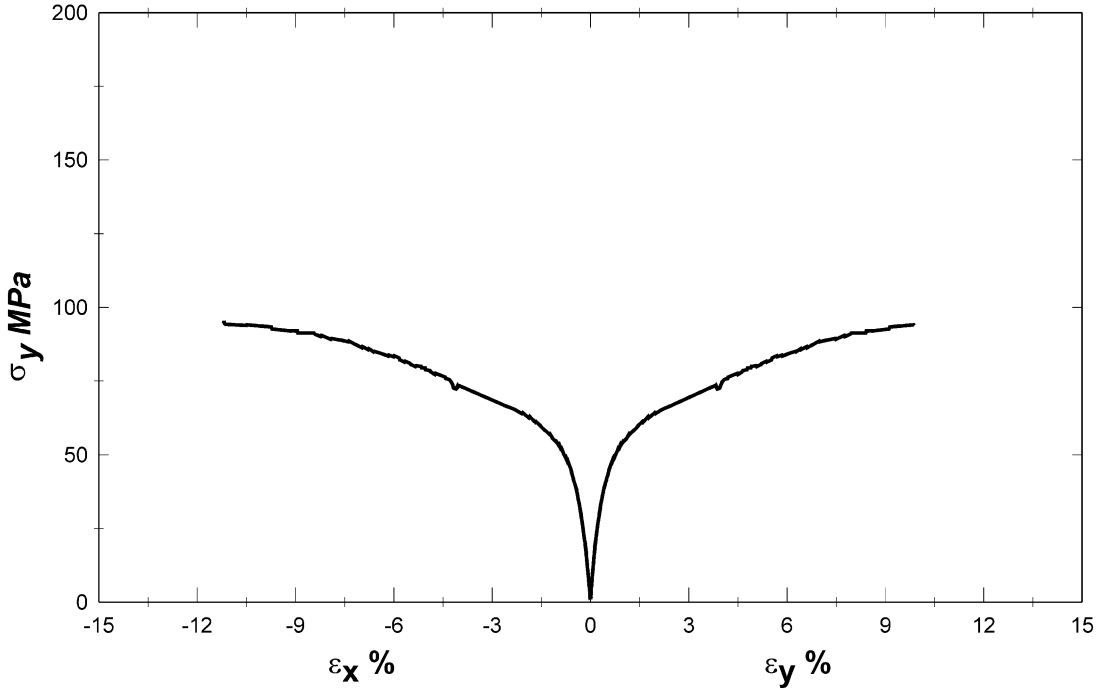

Fig. 14. Typical stress–strain curves for ±45° GRP angle ply laminate made under biaxial tensile loading with σ_y:σ_x = 1:-1.

Table 13
Data for stress–strain curves for ±45° angle ply tubes made of E-glass/epoxy material tested under σ_y:σ_x = 1:−1

Hoop stress σ_y (MPa)	Hoop strain ε_y (%)	Axial strain ε_x (%)
0.0	0.0	0.0
5.59	−0.0402	0.0363
7.11	−0.0520	0.0469
10.07	−0.0749	0.0676
11.13	−0.0863	0.0772
15.02	−0.1156	0.1055
18.83	−0.1503	0.1380
22.30	−0.1955	0.1775
26.69	−0.2474	0.2281
32.22	−0.3246	0.3038
38.22	−0.4248	0.4032
45.10	−0.5961	0.5713
50.47	−0.8205	0.7874
54.57	−1.0404	1.0001
58.13	−1.3764	1.3154
62.97	−1.8534	1.7608
65.37	−2.3117	2.1856
73.47	−4.0114	3.7974
76.35	−4.4314	4.2021
76.48	−4.4583	4.2266
79.49	−5.0472	4.7956
81.44	−5.6688	5.3825
83.81	−6.1527	5.8412
84.88	−6.6135	6.2716
88.87	−7.5960	7.1889
90.97	−8.4206	7.9416
92.01	−8.9463	8.4200
92.70	−9.7163	9.1120
93.92	−10.499	9.8910
94.82	−11.190	

Data for Fig 21 of the failure exercise, data taken from Ref [25].

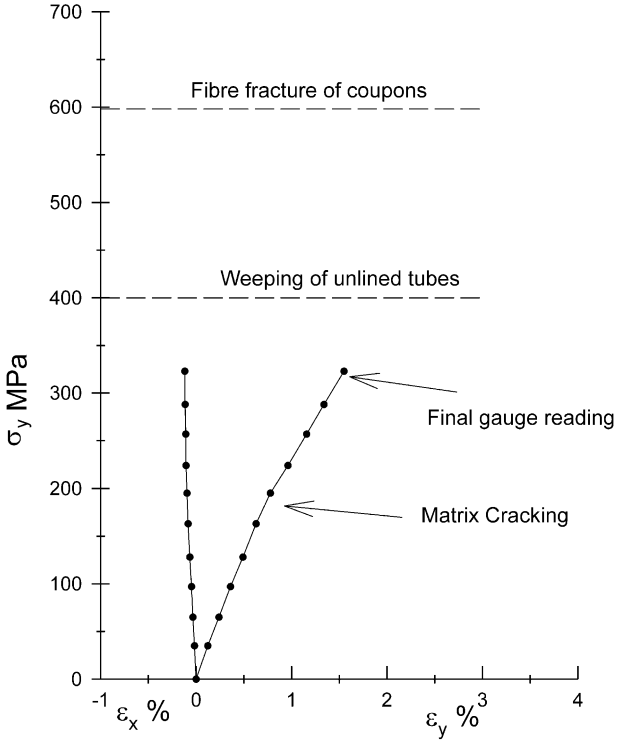

Fig. 15. Stress–strain curves for (0°/90°) GRP cross ply tubes under internal pressure, at σ_y:σ_x = 1:0. Results supplied by Eckold (1997).

the fibre (E_1, υ_{12}, ε^u_{1T}, X_{1T}) were measured using thin walled circumferentially wound tubes subjected to internal pressure using a test rig similar to that shown in Fig. 7(a). The transverse (perpendicular to the fibres) tensile properties (E_2, υ_{21}, ε^u_{2T}, X_{2T}) were measured

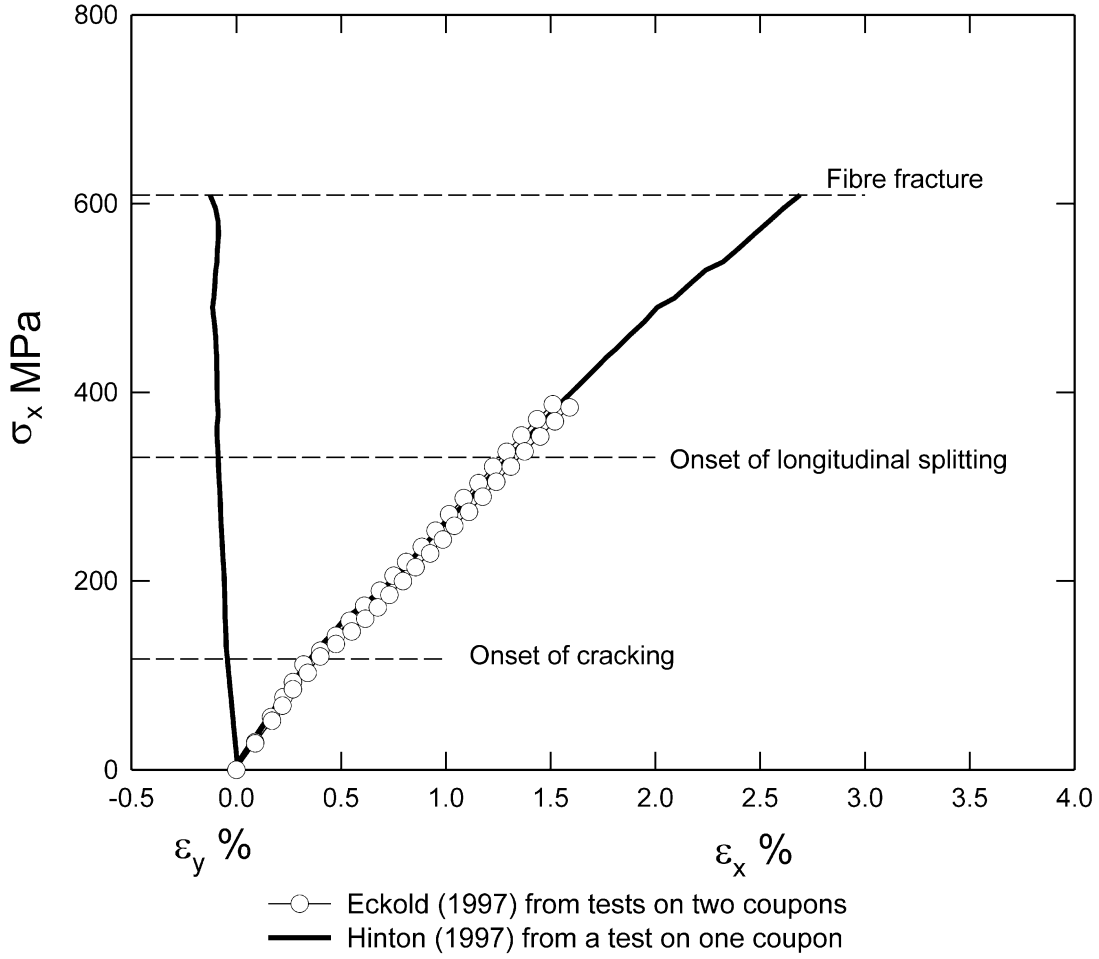

Fig. 16. Typical stress–strain curves for (0°/90°) GRP cross ply coupons under uniaxial tensile loading with σ_x:σ_y = 1:0.

using thin walled circumferentially wound tubes subjected to axial tension. In both cases, the stress–strain curves were linear up to failure.

The longitudinal compressive properties (E_1, υ_{12}, ε^u_{1C}, X_{1C}) were measured using thick blocks of unidirectional lamina under axial compression. The stress–strain curve is linear up to failure. Early work at QinetiQ [32], on pultruded bars of 60% volume fraction, showed that the compressive strength was 520 MPa which agrees with typical values reported elsewhere [33]. However, recently QinetiQ carried out a more thorough investigation on the determination of the longitudinal compressive strength of E-glass/MY750 epoxy. In this recent work [31], using an improved test rig the results show that for high fibre volume fractions of fibres (65–71%), the strength was about 1150MPa. The value of longitudinal compressive strength was scaled to 60% volume fraction to give the value of 800MPa used in this exercise. Further experiments are required to confirm this result.

The transverse compressive properties (E_2, υ_{21}, ε^u_{2C}, X_{2C}) were measured using thick hoop wound tubes under axial compression, Harwood and Hinton [34], and rectangular cross section blocks of UD material [35]. The stress–strain curve exhibits a slight non-linearity as described in Part A of the exercise.

The in-plane shear properties including initial modulus G_{12}, the strength S_{12} and failure strain γ^u_{12} were measured using circumferentially wound tubes under torsion. The stress–strain curve is highly non-linear and Hinton et al. [36], described the non-linearity using a fourth order polynomial.

The thermal expansion coefficients and stress free temperature were measured by Hinton [32], using blocks of UD composite and cross ply laminates, respectively.

Parvizi et al. [37], measured a fracture surface energy for cracks running parallel to the fibres using the work-to-fracture and linear elastic fracture mechanics methods. The specimens used were edge-notched rectangular bars under three-point bending and double notched rectangular specimens under uniaxial tension. They reported a value of 120 ± 30 J/m^2 of the fracture energy for initiation of cracks. Eckold [26], reported a value of 165–185 J/m^2 for the matrix cracking energy for the same composite material. Krawczak and Pabiot [38], measured G_{IC} for E-glass/Epikote 828 epoxy materials using DCB and reported values in the range 87–224 J/

Table 14
Data for stress strain curves for cross-ply (0/90) coupons made of E-glass/epoxy material tested under uniaxial tension

σ_x (MPa)	ε_y (%)	ε_x (%)
0.000	0.000	0.000
6.172	0.005	0.004
22.082	−0.002	0.050
38.143	−0.009	0.099
53.749	−0.016	0.147
68.146	−0.022	0.192
83.140	−0.028	0.240
98.680	−0.035	0.290
114.62	−0.041	0.343
130.49	−0.048	0.397
145.09	−0.050	0.463
159.26	−0.053	0.514
174.37	−0.054	0.607
189.16	−0.056	0.684
205.01	−0.058	0.766
220.17	−0.062	0.826
236.19	−0.067	0.890
251.86	−0.071	0.954
267.80	−0.074	1.023
283.65	−0.076	1.099
299.29	−0.080	1.164
314.89	−0.083	1.228
331.07	−0.086	1.303
345.56	−0.090	1.365
360.79	−0.093	1.428
376.65	−0.086	1.496
392.22	−0.090	1.565
422.74	−0.093	1.703
437.38	−0.094	1.768
446.08	−0.096	1.813
460.34	−0.099	1.877
474.86	−0.105	1.948
489.94	−0.114	2.009
499.77	−0.107	2.091
515.10	−0.102	2.166
529.57	−0.098	2.240
538.10	−0.092	2.322
552.77	−0.090	2.399
567.56	−0.085	2.472
581.42	−0.087	2.544
595.42	−0.099	2.613
609.14	−0.125	2.691

Data for Fig. 23 of the failure exercise. Data supplied by Hinton [29].

m^2 for the initiation mode, depending upon the coupling agent used. Miyase [39] measured the same property for E-glass/ Epon 828 epoxy using a Width Tapered Double Cantilever Beam (WTDCB) and reported an average value of 214 ± 30 J/m^2. For the E-glass/MY750 lamina used in the exercise, the critical strain energy release rate G_{IC} for mode I (delamination mode of deformation) was assumed to be 165 J/m^2, based on the various values mentioned.

3.2. Material II: E-glass/LY556/HT907/DY063

Most of the data for this material presented in Part A were reported in Refs. [1,2,8,40]. The types of fibre and epoxy are rather similar to those of the material I described above and, hence, the properties are also similar. The fracture toughness and thermal expansion coefficients were assumed to be the same as those for material I.

3.3. Material III: T300/BSL914C carbon/epoxy

Most of the data for this material presented in Part A were reported by Schelling and Aoki [3,4]. The shear stress–strain curve was assumed to follow the same behaviour as that of T300/914 epoxy lamina, see Panhwar and Scott [41], Ladeveze and Dantec [42] and Lafarie-Frenot and Touchard [43], and similar laminae (XAS/914C) reported by Sanders and Grant [44]. The thermal expansion coefficients, the stress free temperature and interlaminar fracture toughness were all assumed.

3.4. Material IV: AS4/3501-6 carbon/epoxy

The AS4/3501–6 material comes in the form of prepregs. A typical curing cycle recommended by the suppliers (Hercules) of this material is summarised below, see Dickson et al. [45]

Parameters	**Details**
Initial pressure	56 cm Hg vacum, 568 kPa
Initial heat rise	to 121 °C at 2–3 °C/min
Dwell	60 min at 121 °C
Pressurise	raise pressure to 690 kPa and vent bag
Final heat rise	121–177 °C at 2–3 °C/min
Cure	177–60 °C at 4 °C/min under pressure
Depressurise	release autoclave pressure

Characterisation of the UD properties of AS4/3501-6 was made by a large number of researchers including Swanson and his co-workers [14–19]. The longitudinal tensile properties (E_1, υ_{12}, ε^u_{1T}, X_{1T}) were measured by Colvin and Swanson [17], and Swanson and Trask [19], using coupons under uniaxial tension. The stress–strain curve was reported to exhibit slight stiffening with the modulus varying from $E_{1ini} = 126$ GPa at small strain to $E_{1sec} = 142$ GPa at failure. Work reported by other investigators on various types of CFRP materials confirmed such non-linearity and showed that the secant modulus is 5–15% higher than the initial modulus [46–47].

The transverse tensile properties (E_2, υ_{21}, ε^u_{2T}, X_{2T}) were measured by Swanson and Toombes [48], using coupons subjected to axial tension. The stress–strain curve is linear up to failure.

The uniaxial longitudinal compressive properties (E_1, υ_{12}, ε^u_{1C}, X_{1C}) for AS4/3501-6 CFRP material were measured by a number of workers and frequently different

values of failure strength and failure strain were reported. A scatter as large as 30% in the compressive strength of AS4/3501–6 material obtained from different methods was reported by Abdullah [49], although the coefficients of variations were less than 8% within each test method. Wung and Chatterjee [50], used three test methods and reported a standard deviation in the mean value of compressive strength reaching 28% within one test method. They also obtained mean strength values ranging from 820 to 1179 MPa. Swanson and Nelson [14] and Swanson and Trask [19], reported a strength value of 1190 MPa from axial compression tests carried out on $0^\circ/90^\circ$ cross ply tubes of 96.5 mm diameter and 1.5–2.11 mm thick. Other workers [51,52] have reported values of the compressive strength ranging from 1450 to 2000 MPa. Sun and Jun [53], reported values of X_{1C} of 1100–1750 MPa at various values of volume fractions of fibres ($V_f = 0.5$–0.67), all collected from other published work. The value of the compressive strength was taken as 1480 MPa, Swanson and Nelson [14], for use in the exercise.

The transverse compressive properties (E_2, υ_{21}, ε^u_{2C}, X_{2C}) were measured by Swanson and Toombes [48], using hoop wound tubes under axial compression. The stress–strain curve was reported to be linear. However, Daniel and Ishai [54], showed that the stress–strain curve for the same material in non-linear and the shape of the non-linear curve selected in Part A of the exercise was based upon this. In the latter work, the tests were carried out on coupons.

Other types of carbon/epoxy materials such as IM7/8551–7 [55], T300/LY556 and T800/GY281 [47], HTS/914C [46] and T800/924C [57] also showed non-linear response under transverse compression. For these materials, the final modulus at failure was between 7 and 36% lower than the initial modulus, depending upon the material. The type of matrix and method of curing is likely to have an effect on the degree of non-linearity. It is known that 3501-6 epoxy is brittle [19], while LY556/HT976 epoxy could be fairly ductile, depending upon the curing procedure [47].

The in-plane shear properties including initial modulus G_{12}, the strength S_{12} and failure strain γ^u_{12} were measured using different test specimens and the results were presented by Swanson et al. [20,48,58,59], and other investigators. Swanson and his co-workers used three types of specimens under different types of loadings (1) 90° hoop wound tubes under torsion [58], (2) Iosipescu specimens (notched beam under four point bending) [58], and (3) ($\pm 45^\circ$) tubes under internal pressure [20,48]. They reported that the stress–strain curve is highly non-linear and that the values of failure strain and strength depend on the test specimen, although the initial modulus was almost the same in all cases. The typical shear stress–strain curve selected for the material taken from Swanson and Toombes [48], for tests on unidirectional lamina under torsion. The curve is in agreement with that published by Daniel and Ishai [54], which was obtained from tests on $\pm 45^\circ$ and 10° off-axis coupons. The failure strain in the work of Daniel and Ishai [54], was less than that specified in Part A which was 2%, taken from [48]. The failure strain specified is smaller than that reported by Swanson et al. [58].

The value of shear strength for AS4/3501–6 was chosen to be 79 MPa [48]. This value was slightly lower than a previous value of 96 MPa which was obtained from torsion and Iosipescu specimens and was published by Swanson et al. [58]. Other published values [51–53,65], are in the range of 71–110 MPa, depending upon the test method.

The thermal expansion coefficients and the curing temperature were reported by Kim and Castro [51], Lee and Daniel [60], Daniel and Ishai [54], and others.

The critical strain energy release rate G_{IC} for AS4/3501-6 material was taken as 220 J/m^2. G_{IC} was measured by many investigators using double cantilever beam (DCB) specimens. The results ranged from 137 to 260 J/m^2, see Daniel et al. [61], Smiley and Pipes [62], Rybicki et al. [63], and Yaniv and Daniel [64]. Long and Swanson [66], gave a value of 136 J/m^2, based upon a communication with Hercules Inc (AS4/3601–6 material manufacturer).

4. Laminate models

The composite specimens from which the experimental results were obtained did not have exactly the same structure as the models specified for analysis. All of the models were symmetric laminates with a small number of layers. Almost all of the specimens were tubes and were made by hand lay up or filament winding. The exact dimensions of the test specimens have been described in Section 3. Some of the major differences between the models given in Part A and the actual test pieces are highlighted below.

The helical filament winding process results in a rather complex interwoven structure (see for example Jones and Hull [67]). One complete cover produces one $+\theta$ layer and one $-\theta$ layer at each point on the tube, but the layer sequence can be reversed at different positions. In a filament wound tube with more than one cover the $+\theta$ and the $-\theta$ layers occur alternately throughout the wall of the tube.

The thicker filament wound tubes (>2 covers) have more layers than the corresponding theoretical models. For example, the ($90^\circ/\pm 30^\circ/90^\circ$) glass/epoxy filament wound tube would have more than two $\pm 30^\circ$ covers to make up the required wall thickness giving more than the two $+30^\circ$ and two -30° layers assumed in the model.

The quasi isotropic $(90^\circ/\pm 45^\circ/0^\circ)_s$ carbon/epoxy tubes used in the experiments were made by hand lay

up. The majority of those tubes had the same 8 layer symmetric laminate arrangement specified for the model but thicker tubes had more (3 or 4) repetitions of the 4 layer sequence.

In the experiments the tubular test specimen geometry applies constraints on the deformation of the laminate. Axisymmetric deformation of a thin cylindrical shell under uniformly distributed loading gives rise to the following constraints on bending (K_x and K_y) and twisting (K_{xy}) curvatures:

$$K_x = \mathrm{d}^2 w/\mathrm{dx}^2 \tag{5}$$

$$K_Y = 0 \tag{6}$$

$$K_{xy} = \gamma_{xy}/\mathrm{R} \tag{7}$$

(where w is radial displacement, γ_{xy} is the in-plane shear strain and× is axial co-ordinate.)

The two cover $\pm 55^\circ$ filament wound glass/epoxy specimens had a layer sequence of $+55/-55/+55/-55$, or the reverse, at any given point on the tube (see above). An unconstrained laminated plate of such construction would twist under the action of in-plane normal loading, giving a slightly different stress distribution from the symmetric model. For a balanced laminate (i.e. a laminate with equal $+\theta$ and $-\theta$ layers) shear strain would only occur if shear or bending loads were applied.

For a tubular specimen loaded only by normal loads, the stresses experienced by the tube wall remote from its ends could be simulated by a plate of the same balanced antisymmetric laminated construction, constrained so that the three bending and twisting curvatures [Eqs. (5)–(7)] are zero.

To avoid introducing such complications in Part A of the exercise all laminates were specified as symmetric, which is an alternative way of simulating tube behaviour.

In thicker walled filament wound tubes with more covers (e.g. the $\pm 55^\circ$ filament wound tubes tested under compression and the $\pm 45^\circ$ filament wound tubes tested at **SR** = 1:−1) the effects of direct load/twisting coupling would be negligible because their walls were constructed from many layers but the overall wall thicknesses were greater than those of the models.

One difference between the symmetric laminate models and the antisymmetric structure of the filament wound tubes which should be noted is the difference between the effective thickness of the middle layers. The $0^\circ/90^\circ$ specimens had the same arrangement as the theoretical model which had a thick central layer. The antisymmetric structure of the two cover filament wound $\pm 55^\circ$ and $\pm 45^\circ$ tubes used in the biaxial tension tests gave four layers of equal thickness but the symmetric 4 layer angle ply models specified for those cases had two adjacent layers at the same angle, resulting in an equivalent central layer of double thickness which could be predicted to behave differently by some theories.

The $\pm 55^\circ$ and $\pm 45^\circ$ Glass fiber/epoxy tubular specimens were designed using linear elastic thin shell theory. Recent nonlinear theoretical analysis has indicated that the 60 mm gauge length was too short for the $\pm 45^\circ$ specimens. A more rigorous analysis of the stresses in tubular specimens requires allowance for large displacements and non-linear material properties. The appendix, that was issued with the experimental results, contains a single sample problem which contributors with integrated laminate failure analysis and finite element packages could use to demonstrate a more complete analysis of tubular specimen behaviour.

Uniaxial or biaxial loading was specified for analysis of the theoretical models. In the experiments the tubes were frequently loaded under internal or external pressure. The pressure produces radial compressive stress on one surface but the other surface has no radial stress applied. In thin walled tubes (e.g. the 1 mm thick, 100 mm diameter tubes) the effects of the radial stress are assumed to be negligible (Al-Khalil et al. [5]). Under some conditions (e.g. biaxial compression, Table 6) it was necessary to use thick walled tubes to avoid buckling. In such cases the stresses are not uniform throughout the thickness of the tube. Very high external pressures (up to 200 MPa) were required to fracture some of the tubes but the most severe stress conditions appear to be at the inside surface where the circumferential stress was maximum and the radial stress was zero [10].

5. Conclusions

1. The wide range of experimental results selected for comparison with the theoretical predictions in Part B of the Exercise have been presented.
2. We have tried to draw attention to limitations in some of the experiments and results. The results are subject to error and more and better experimental data are desirable in some cases.
3. The source of data and the methods used in deriving the material properties for the unidirectional laminae and constituents use in part A of the exercise have been outlined.
4. Differences between the symmetric laminated plate models used in the theoretical analysis and the tubular test specimens have been discussed.
5. Comparisons between the theoretical predictions and the wide range of experimental data should help identity any major discrepancies, limitations and areas requiring further theoretical and experimental work.

Acknowledgements

Some of this work was sponsored by Technology Group 04 of the UK MoD Corporate Research Programme and by Department of Trade and Industry (DTI) in the United Kingdom.

Appendix

Details of the specimen to be analyzed in Part B

As pointed out in the instructions for Part A, the organizers are asking those participants who have integrated failure analyses and structural analysis packages if they wish to analyze a simple structure. The following section gives details of the simple structure proposed. Identical details are distributed to all participants.

Structure to be analyzed

Figs. (A1) and (A2) show details of the tubular specimen to be analyzed in Part B of the exercise.

Material and dimensions

The tube is 100 mm inside diameter, 1 mm thick and 283 mm long and made of E-glass/MY750 epoxy material with fiber volume fraction of 60%. The properties for this material (Material I) were sent previously to all contributors.

Lay-up

The tube is made of four plies oriented at $+55°/-55°/+55°/-55°$ with respect to the tube axis. All the plies have an equal thickness of 0.25 mm.

End Reinforcement

Reinforcement is applied along a distance of 111.5 mm from each end of the specimen, leaving a section, 60 mm long, in the middle of the tube without reinforcement. The end reinforcement is in the form of circumferentially wound glass/epoxy material identical to the material of the tube (E-glass/ MY750 epoxy). Two shapes are shown in Fig. (A2) for the end reinforcement (i) a stepped shape representing the state of the as-manufactured reinforcement and (ii) an approximate shape, broken line in Fig. (A2), with a radius of 298 mm, tangential to the outside surface of the tube at the end of the 1 mm thick test section. Either of these forms of reinforcement can be used in your analysis.

Loading

The tube is subjected to a uniform internal pressure along a length of 213 mm. The tube is free at its two ends and no axial end load or pressure is applied.

Results

Please plot a graph showing stress versus circumferential and axial strains on the outside surface of the tube at the center of the gauge length as the pressure

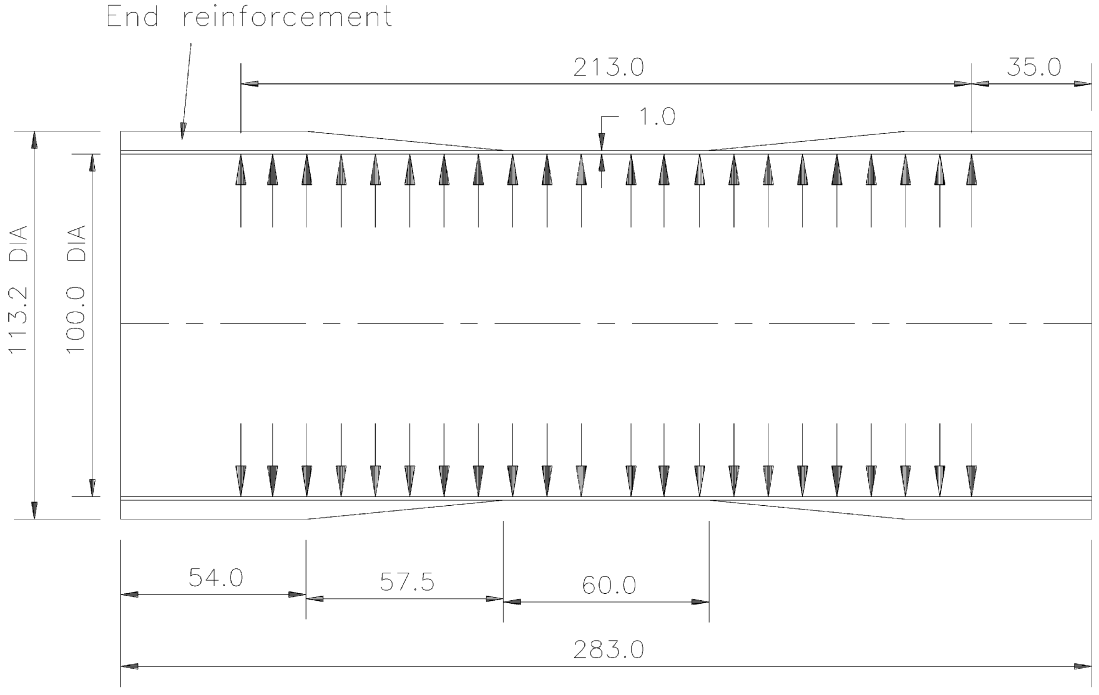

Fig. A1. Geometry of the tubular specimen. (Inner diameter = 100 mm, thickness = 1 mm, overall length = 283.0 mm).

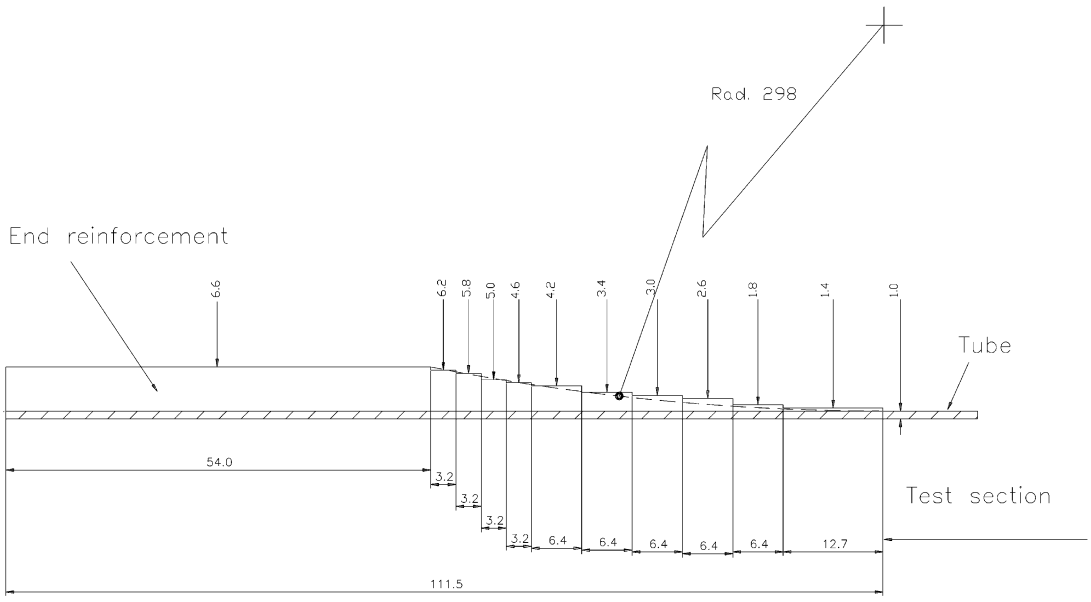

Fig. A2. Details of end reinforcement geometry of a 55 GRP composite tube. Dimensions are in mm.

increased up to the final failure. Use the scales provided previously in Fig. 16 of Part A. These results can then be compared with your previous prediction and the experimental results provided for Part B, Fig. 8.

Also, please report the circumferential and axial stresses at the inside and outside surfaces of the tube at the center of gauge length at the final failure pressure.

Contributors may also choose to plot a figure or figures in their favoured format to demonstrate the development of failure in the specimen.

References

[1] Hütter U, Schelling H, Krauss H, An experimental study to determine failure envelope of composite materials with tubular specimen under combined loads and comparison between several classical criteria. In: Failure Modes Of Composite Materials With Organic Matrices And Other Consequences On Design, NATO, AGRAD, Conf Proc No. 163, Munich, Germany, 13–19 October 1974.

[2] Krauss H, Schelling H. Kunststffe 1969;59(12):911–7.

[3] Schelling H, Aoki RM, DFVLR, Germany, Personal communication; 1992.

[4] (ZTL80) Dornier, Fokker, MBB, DLR: Investigations of Fracture Criteria of Laminae. 1975–1980, BMVg [multiaxial testing, reports in German].

[5] Al-Khalil MFS, Soden PD, Kitching R, Hinton MJ. The effects of radial stresses on the strength of thin walled filament wound GRP composite pressure cylinders. Int J Mech Sci 1996;38:97–120.

[6] Soden PD, Kitching R, Tse PC. Experimental failure stresses for $\pm 55^{\circ}$ filament wound glass fibre reinforced plastic tubes under biaxial loads. Composites 1989;20:125–35.

[7] Soden PD, Kitching R, Tse PC, Tsavalas Y, Hinton MJ. Influence of winding angle on the strength and deformation of filament wound composite tubes subjected to uniaxial and biaxial loads. Compos Sci Tech 1993;46:363–78.

[8] Forster R, Knappe W. Kunststoffe 1970;60(12):1053.

[9] Kaddour AS, Soden PD. Design of a high pressure rig for biaxial and triaxial compression testing of composite tubes. Science and Engineering of Composite Materials 1996;5:27–38.

[10] Kaddour AS, Soden PD, Hinton MJ. Failure of $\pm 55^{\circ}$ filament wound composite tubes under biaxial compression. J Compos Mater 1998;32(18):1618–45.

[11] Al-Khalil M F S, Strength of filament wound structure under complex loading. PhD thesis, UMIST, England; 1990.

[12] Al-Salehi FAR, Al-Hassani STS, Hinton MJ. An experimental investigation into the strength of angle GRP tubes under high rate of loading. J Comp Mater 1989;23:288–305.

[13] Kaddour AS, Soden PD, Hinton MJ, Unpublished work; 1996.

[14] Swanson SR, Nelson M. Failure properties of carbon/epoxy laminates under tension-compression biaxial stress. In: Kawata K, Umekawa S, Kobayashi A. Composites '86: Recent Advances in Japan and United States, Proc Japan-US CCM-III, Tokyo, Japan; 1986. p. 279–86.

[15] Swanson SR, Christoforou AP. Response of quasi-isotropic carbon/epoxy laminates to biaxial stress. J Compos Mater 1986;20:457–71.

[16] Swanson SR, Colvin GE. Compressive strength of carbon/epoxy laminates under multiaxial stress. Final annual report to the Lawrance Livermore National Laboratory, UCRL-21235; 1989.

[17] Colvin GE, Swanson SR. In situ compressive strength of carbon/epoxy AS4/ -6 laminates. J Eng Mater Tech 1993;115:122–8.

[18] Swanson SR, Christoforou AP, Colvin GE. Biaxial testing of fibre composites using tubular specimens. Exp Mech 1988;28:238–43.

[19] Trask BN, Response of carbon/epoxy laminates to biaxial stress: MSc thesis, Department of mechanical and Industrial Engineering, The University of Utah, Utah, USA; 1987.

[20] Swanson SR, Christoforou AP. Progressive failure in carbon/epoxy laminates under biaxial stress. Trans ASME, J Eng Mater Technol 1987;109:12 –16, .

[21] Christoforou AP, MSc thesis, Department of Mechanical and Industrial Engineering, the University of Utah, Utah, USA; 1984.

[22] Swanson SR, Trask BC. Strength of quasi-isotropic laminates under off-axis loading. Compos Sci Technol 1989;34:19–34.

[23] Li S. Modelling damage in thin walld filament wound structures. Manchester, UK: PhD thesis UMIST; 1993.

[24] Reid SR, Soden PD, Li S. Application of damage models to filament wound tubes. MoD Final Report, Contact No 2044/186; 1995.

[25] Kaddour AS, Soden PD and Hinton MJ. Quasi-static behaviour of ±45° glass/epoxy filament wound composite tubes under equal biaxial tension-compression loading: experimental results: to be published.
[26] Eckold GC. The effect of damage on the mechanical properties of composites and its impact on design. IMechE Conference Designing out Failure in Composites, held at London UK, 23 September 1994.
[27] Eckold GC, Hancox NL, Lee RJ. Application of micromechanics in the prediction of damage initiation and growth in structural composites. In: 3rd Int. Conf. on Deformation and Fracture of Composites, Institute of Materials, University of Surrey, Guilford, UK, 27–29 March 1995. p. 66–76.
[28] Eckold GC. Personal communication; 1997.
[29] Hinton MJ. Private communication; 1997.
[30] Soden PD, Hinton MJ, Kaddour AS. Lamina properties, lay-up configurations and loading conditions for a range of fibre reinforced composite laminates. Compo Sci Technol 1011;58:1998.
[31] Hinton MJ. Private communication; 1995.
[32] Hinton MJ. RARDE report; 1978.
[33] Tsai SW. Theory of composites design, Think Composites. Palo Alto; 1992.
[34] Harwood CK and Hinton MJ. Investigation of the transverse compression properties of glass fibre/epoxy resin system using circumferentially wound tubes. RARDE, Memorandum 38/79 (EM4), MoD, UK; 1979.
[35] Jones RM Mechanical properties of GRP in the through thickness. MSc dissertation, UMIST, Manchester, UK; 1986.
[36] Hinton MJ, Soden PD, Kaddour AS. Strength of composite laminates under biaxial loads. Applied Composite Materials 1996;3:151–62.
[37] Parvisi A, Garrett KW, Bailey JE. Constrained cracking in glass fibre reinforced epoxy cross ply laminates. J Mater Sci 1978;13: 195–201.
[38] Krawczac P, Pabiol J. Fracture mechanics applied to glass fibre/epoxy matrix interface characterization. Journal of Composite Materials 1995;29:2230–53.
[39] Miyase A. Transverse tensile strength anisotropy in thick filament wound ring composites. J Mater Sci 1984;19:923–8.
[40] Forster R. Kunststoffe 1972;62(1):57–62.
[41] Panhwar NM, Scott ML. Shear fatigue performance of post-buckling fibre composite panels. ICCM-9 1993;I:527–34.
[42] Ladevese P, Le Dantec E. Damage modelling of the elementary ply for laminated composites. Compo Sci Techno 1992;43:257–67.
[43] Lafarie-Fernot MC, Touchard F. Comparative in-plane shear behaviour of long carbon-fibre composites with thermoset or thermoplastic matrix. Compo Sci Technol 1994;52:417–25.
[44] Sanders RC, Grant P. The strength of laminated plates under in-plane loading, Part 1: failure criteria. Report SOR (P) 130, BAe, Warton Aerodrome, Preston, UK.
[45] Dickson T, Munro M, Lee S. Selection of an-plane shear test method based on the shear sensitivity of laminate tensile modulus. Composites 1995;26:17–24.
[46] Ditcher AK, Rhodes FE, Webber JPH. Non-linear stress–strain behaviour of carbon fibre reinforced plastic laminates. J Strain Analysis 1981;16:43–51.
[47] Schulein R, Keinzler J, Scharr G, Hackenberg R, Aoki R. Verbesserung der ausnutzbarkeit der neuen hochfesten C-fasern in hochbelastelen verbubdstrukturen und verbesserung des dimensionierungsverfahrens, VDI Fortuschritt Berichte, Reihe 5, Nr 186. Dusseldorf, VDI-Verlag; 1989.
[48] Swanson SR, Toombes GR. Characterisation of prepreg tow carbon/epoxy laminates. J Engg Mater Techno, Trans ASME 1989;111:150–3.
[49] Abdullah MG. State of the art of advanced composite materials: compression test methods. JANNAF, CMGS, and S &MBJ Joint Meeting, 27–30 November 1994, Jet Propulsion Lab., California Institute of Technology, Pasadena, CA; 1994.
[50] Wung ECJ, Chatterjee SN. On the failure mechanisms in laminate compression specimens and the measurement of strengths. J Compos Mater 1992;26:1885–914.
[51] Kim R, Castro AS. A longitudinal compression test for composites using a sandwitch specimen. J Compos Mater 1992;26:1915–29.
[52] Daniel IM, Hsiao HM, Wooh SC, Vittoser J. In: AMD, vol 162, mechanics of thick composites. ASME publication; 1993. p. 107–26.
[53] Sun CT, Jun AW. Effect of matrix non-linear behaviour on the compressive strength of fibre composites. In AMD, vol 162, mechanics of thick composites. ASME; 1993, p. 91–105.
[54] Daniel IM, Ishai O. Engineering mechanics of composite materials. Oxford, UK: Oxford University Press; 1994.
[55] Colvin GE, Swanson SR. Mechanical characterization of IM7/ -7 carbon/epoxy under biaxial stress. J Engg Mater Techno 1990; 112:61–7.
[57] Jelf PM, Fleck NA. The failure of composite tubes due to combined compression and torsion. J Mater Sci 1994;29:3080–4.
[58] Swanson SR, Messick MJ, Toombes GR. Comparison of torsion tube and Iosipescu in-plane shear test results for a carbon fibre reinforced epoxy composite. Composites 1985;16:220–4.
[59] Swanson SR, Messick MJ, Tian Z. Failure of carbon/epoxy lamina under combined stress. J Comp Mater 1987;21:619–30.
[60] Lee J-W, Daniel IM. J Compos Mater 1990;24:1225.
[61] Daniel IM, Yaniv G, Auser JW. Rate effects on delamination fracture toughness of graphite epoxy composites. In: ICCS/4, Paisley College of Technology, Scotland, 27–29 July 1987. p. 2.258–2.272, 1987.
[62] Smiley AJ, Pipes RB. Rate effects on Mode I interlaminar fracture toughness in composite materials. J Compos Mater 1987;21: 670–87.
[63] Rybicki E, Herenandez TD, Dileber JE, Knight RC, Vinson SS. Mode I and mixed mode energy release rate values for delamination of graphite/epoxy test specimens. J Compos Mater 1987; 21:105–23.
[64] Yaniv G, Daniel IM. In: Whitcomb JD, editor. High-tapered double cantilever beam specimen for study of rate effects on fracture toughness of composites. ASTM STP 972, Philadelphia, USA; 1988. p. 241–258.
[65] Sun CT, Zhou SG. Failure of quasi-isotropic composite laminates with free edges. J Reinf Plast Compos 1988;7:515–57.
[66] Long BJ, Swanson SR. Ranking of laminates for edge delamination resistance. Composites 1994;25:183–8.
[67] Jones MLC, Hull D. Microscopy of failure mechanisms in filament wound pipe. J Mater Sci 1979;14:165–77.
[68] Carroll M, Ellyin F, Kujawski D, Chiu AS. The rate dependent behaviour of ±55° filament wound glass fibre/epoxy tubes under biaxial loading. Compo Sci Technol 1995;55:391–403.
[69] Aliutov NA, Zinoviev PA. Deformation and failure of fibrous composites with brittle polymeric matrix under plane stress. In: Mechanics of Composites. MIR publishers, Moscow; 1982.